

Astronomy & Astrophysics manuscript no.
(will be inserted by hand later)

Measuring age, metallicity and abundance ratios from absorption line indices

Rosaria Tantalo and Cesare Chiosi

Department of Astronomy, University of Padova, Vicolo dell'Osservatorio 2, 35122 Padova, Italy
e-mail: tantalo@pd.astro.it; chiosi@pd.astro.it

Received: August, 2001; revised: November 2002; accepted ***

Abstract. In this study we present detailed calculations of absorption line indices on the Lick System, e.g. H_{α} , Mg_{β} , Mg_{γ} , $hFeI$, NaD and C_24668 , based on the new stellar models by Salasnich et al. (2000) that incorporate the enhancement of elements both in the opacity and in the chemical abundances. The stellar models span large ranges of initial masses, chemical compositions, and ages. They are followed from the zero age main sequence till the end of the asymptotic giant branch phase or carbon ignition as appropriate, and are calculated for both solar-scaled and enhanced abundance patterns. Using these models and the calibration by Tripicco & Bell (1995), we calculate the integrated indices of Single Stellar Populations (SSPs) of different age, metallicity and degree of enhancement in the elements. Finally, with the aid of the triplet H_{α} , Mg_{β} and $hFeI$, and the Minimum-D instance method proposed by Trager et al. (2000b), we derive the age, metallicity and enhancement degree for the galaxies of the Gonzalez (1993) sample and compare the results with those by Trager et al. (2000b). Since very large differences are found, we analyze in a great detail all possible sources of disagreement, going from the stellar models and SSPs in use to the pattern of chemical elements (especially when enhanced mixtures are adopted), and the technical procedure used to extend grids of existing theoretical indices. We find that each of the above aspects of the problem bears very much on the final result. Amazingly enough, at increasing complexity of the underlying stellar models and SSPs, the uncertainty of the whole procedure and final results increases. We also analyze how the determinations of age, metallicity and degree of enhancement change at varying the indices under considerations. To this aim we turn to the Trager 'IDSP pristine' sample which contains many more galaxies and a much wider list of indices than in the Gonzalez sample. The solutions (age, metallicity, degree of enhancement) we find using different triplets of indices are not unique in that reflecting the poor ability of most indices to disentangle age from metallicity. We also try to better constrain the result by simultaneously using six indices (H_{α} , Mg_{β} , Mg_{γ} , $hFeI$, NaD and C_24668). Finally, starting from the hint that C_24668 and NaD , seem to depend strongly on the metallicity and degree of enhancement and weakly on the age, we propose a new method, i.e. the Recursive Minimum-D instance method, to break the age-metallicity degeneracy and to stabilize the solution for age, metallicity, and degree of enhancement. We also make some remarks on the popular two-indices diagnostic. The main conclusion of this study is that deriving ages, metallicities and degree of enhancement from line indices is a cumbersome affair whose results are uncertain. The difficulty may be perhaps overcome only if special care is paid to the quality of the underlying stellar models and the solving procedure.

Key words. Galaxies: elliptical & galaxies: chemical evolution & Galaxies: metallicities & Galaxies: ages & Galaxies: photometry

1. Introduction

Over the years, much effort has been spent to infer from observational data the age, metallicity, and enhancement of the elements of the stellar content in early-type galaxies (EGs) (Bressan et al. 1996; Tantalo 1998; Tantalo et al. 1998a; Trager et al. 2000b,a; Jorgensen 1999; Kuntschner 2000; Kuntschner et al. 2001; Vazdekis et al. 2001; Davies et al. 2001).

Determining the age and metallicity is a cumbersome affair hampered by the fact that the spectral energy distribution of an old metal-poor stellar population may happen to be the same of a young metal-rich one. This is otherwise known as the age-metallicity degeneracy pointed out long ago by Renzini & Buzzoni (1986).

A promising way-out is perhaps offered by the absorption line indices defined by the Lick group (Worley 1992; Worley et al. 1994), which seem to have the potential of partially resolving the age-metallicity degeneracy. An extensive use of the two indices diagnostics is currently

made in order to infer the age and the metallicity of early type galaxies (Kuntschner & Davies 1998; Jorgensen 1999; Kuntschner 1998, 2000; Kuntschner et al. 2001; Trager et al. 2000b; Vazdekis et al. 2001; Davies et al. 2001; Poggianti et al. 2001).

The problem is, however, further complicated by a third parameter, i.e. the abundance ratio $[=Fe]$ (where $=$ stands for all chemical elements produced by α -captures on lighter nuclei). Absorption line indices like $M g_2$ and $hFeI$ measured in the central regions of galaxies are known to vary passing from one galaxy to another (Gonzalez 1993; Trager et al. 2000b,a). Looking at the correlation between $M g_2$ and $hFeI$ (or similar indices) for the galaxies in the above quoted samples, $M g_2$ increases faster than $hFeI$, which is interpreted as due to enhancement of α -elements in some galaxies. In addition to this, since the classical paper by Burstein et al. (1988), the index $M g_2$ is known to increase with the velocity dispersion (and hence mass and luminosity) of the galaxy. Standing on this body of data the conviction arose that the degree of enhancement in α -elements ought to increase passing from dwarf to massive EGs (Faber et al. 1992; Worthey et al. 1994; Matteucci 1994, 1997; Matteucci et al. 1998). The simplest and most widely accepted interpretation is the one based on the different duration of the star forming period and the different contribution to α -elements and Fe by Type II supernovae from massive stars (mostly producing α -elements) and Type Ia supernovae from accreting white dwarfs in binary systems (mostly generating Fe). Since the minimum mean time scale for a binary mass-accreting white dwarf to get the supernova stage is 0.5 Gyr, the iron contamination by Type Ia supernovae occurs later as compared to the ones of Type II (Greggio & Renzini 1983). With the standard supernova driven galactic wind model (SDGW) by Larson (1974) and classical initial mass function, to reproduce the observed trend of the $[Fe/mass]$ relationship, the total duration of the star forming activity ought to decrease at increasing galaxy mass. Long ago Larson (1974) suggested that the CMR stems from a mass-mean metallicity relation, whereby the massive EGs are more metal-rich. He also proposed the SDGW mechanism as the key process by which massive EGs, owing to their deeper gravitational potential, retain gas and form stars for longer periods of time than the low-mass ones. This is the opposite of what implied by the trend in α -elements. The kind of behavior for the star formation history in EGs required by the enhancement has been suggested by Bressan et al. (1996); Tantalo et al. (1998a) on the base of their properties in the two indices planes, and more recently confirmed by Poggianti et al. (2001) and the N-body-Tree-SPH models of EGs by Chiosi & Carraro (2002).

In presence of α -enhanced chemical compositions, ages and metallicities of EGs should be derived from indices in which this effect is taken into account. As long ago noticed by Worthey et al. (1992) and Weiss et al. (1995), indices for α -enhanced chemical mixtures of given total metallicity are expected to differ from those of the standard case.

The first attempt to simultaneously derive ages, metallicity and $[=Fe]$ ratios for the early type galaxies of the Gonzalez (1993) sample is by Tantalo et al. (1998a) by means of the so-called α -M method in which the effect of different ratios $[=Fe]$ on theoretical indices has been included assuming the Borges et al. (1995) calibration for $M g_2$ and a suitable relationship between total metallicity Z and iron content $[Fe/H]$ (Bressan et al. 1996; Tantalo et al. 1998a). Similar attempt was made by Trager et al. (2000b, TFWG00) using different calibrations (Tripicco & Bell 1995) but reaching similar results.

However, the SSPs adopted by Bressan et al. (1996); Tantalo (1998); Tantalo et al. (1998a) and also Tantalo et al. (1998b) were actually calculated from the Padova library of stellar models with solar partition of elements and old opacities (Bertelli et al. 1994) and the classical recipe for mass-loss during the red giant branch (RGB) and asymptotic giant branch (AGB) phases. The only major difference in the SSPs of Tantalo (1998); Tantalo et al. (1998a,b) that have been described for the first time in the data base for galaxy evolution models by Leitherer et al. (1996), is the mass-loss rate during the AGB phase for which the formulation by Vassiliadis & Wood (1993) was adopted. In the following we will refer to these SSPs as the Tantalo's version of the Padova SSPs, shortly indicated as TP96. The SSPs adopted by TFWG00 are taken from the even older SSP library by Worthey (1994). In the meantime more recent stellar models, isochrones, and SSPs with improved physical input and α -enhanced chemical mixtures have become available (Salasnich et al. 2000, SGWC00). Therefore, we seek here to improve upon this point of weakness of the previous analyses and also to clarify the role played by different α -enhanced stellar models and/or SSPs. It is worth recalling here the recent studies by Thomasson et al. (2003) and Maraston et al. (2003) on the synthesis of absorption line indices on the Lick system for SSPs with variable chemical abundances and their calibration on a sample of Milky Way Globular Clusters whose metallicities vary from $Z = 30$ to $Z = 1$. Many of the results presented in our study are common to those by Thomasson et al. (2003) and Maraston et al. (2003)¹.

The plan of the paper is as follows. Section 2 defines the so-called enhancement factor for a mixture in which the abundance of α -elements with respect to that of Fe is enhanced as compared to the SolarMix. Section 3 presents a brief description of the new stellar models and SSPs by SGWC00 in which α -enhanced chemical abundances are adopted. Section 4 shortly introduces the definition of the absorption line indices for a single star, and their corresponding integrated values for SSPs. Section 5 presents three different ways of "calibrations" to include the effect of α -enhanced chemical compositions on absorption line indices and the choice we have made. Section 6 describes the formalism we have used to derive the integrated indices

¹ The first version of this paper has been submitted to A&A on August 2001, long before the publication of the studies by Thomasson et al. (2003) and Maraston et al. (2003).

for SSPs. Section 7 first presents the indices for SSPs of different age, metallicity and enhancement factor, second illustrates the method to derive these parameters from the observational indices, finally presents some preliminary results for a selected sample of EGSs and compares them with those from previous studies. Since very large differences are found, in Section 8 we analyze in detail the many reasons why such large differences may occur, i.e. the stellar models in use, the patterns of abundances for enhanced mixtures, and the technique adopted to extrapolate existing grids of theoretical SSPs. In Section 9 we examine whether the solution for the age, metallicity and enhancement factor is unique, in the sense that the same result is obtained using different combinations of indices in groups of three. As expected no unique answer is found. To overcome the difficulty first we check whether imposing the simultaneous fit of many indices the solution can be better constrained, and then in Section 10 we propose a plausible way out based on an iterative procedure standing on the different response of the indices to age, metallicity and degree of enhancement. In Section 11 we draw some remarks on the widely adopted two-indices plane diagnostics to estimate the age, metallicity, and degree of enhancement of elements. Finally, a summary of the results of this study and some concluding remarks are presented in Section 12.

2. Definition of the enhancement factor

In presence of enhancement in elements one has to modify the relationship between the total metallicity Z and the iron content $[Fe/H]$. This is made by suitably defining the enhancement factor ϵ .

Following Tantalo et al. (1998a), let us split the metallicity Z in the sum of two terms

$$Z = \sum_j X_j + X_{Fe} \quad (1)$$

where X_j are the abundances by mass of all heavy elements but Fe, and X_{Fe} is the same for Fe. Recasting eq. (1) as

$$Z = \frac{X_{Fe}}{X_H} X_H + \frac{\sum_j X_j}{X_{Fe}} \quad (2)$$

and normalizing it to the solar values we get

$$\frac{Z}{Z_{\odot}} = \frac{X_{Fe}}{X_H} \frac{X_H}{X_{Fe}} \frac{X_H}{X_H} \frac{h + \frac{p}{h} \frac{\sum_j X_j}{X_{Fe}}}{1 + \frac{p}{h} \frac{\sum_j X_j}{X_{Fe}}} \quad (3)$$

from which we finally obtain

$$[Fe/H] = \log(Z/Z_{\odot}) - \log(X/X_{\odot}) \quad (4)$$

For solar metallicity Z and solar-scaled mixture ($\epsilon = 0$) eq. (4) yields $[Fe/H] = 0$. The definition of ϵ is obvious. This relation is useful to re-scale the Fe content in presence

Table 1. The $[Fe/H]$ ratio for solar-scaled and ϵ -enhanced mixtures as a function of the initial chemical composition $[X, Y, Z]$.

Z	Y	X	$[Fe/H]$	$[Fe/H]$	$[Fe/H]$
0.008	0.248	0.7440	0.3972	0.7529	0.8972
0.019	0.273	0.7080	0.0000	0.3557	0.5000
0.040	0.320	0.6400	0.3672	0.0115	0.1328
0.070	0.338	0.5430	0.6824	0.3267	0.1715

of $\epsilon < 0$ and vice-versa. Therein after ϵ is referred to as the enhancement factor.

In general, when dealing with enhanced chemical mixtures, it succeeds to determine ϵ according to the degree of enhancement and simply re-scale the zero-point for the iron content of the Sun, i.e. $[Fe/H] = \epsilon$. Remarkably, enhancing elements simply reduces to decreasing $[Fe/H]$.

A slightly different definition of enhancement has been adopted by Thomas et al. (2003) which however is fully equivalent to ours so that straight comparison is possible.

3. Stellar models with ϵ -enhanced mixtures

SGWC00 have presented four sets of stellar models with different initial chemical compositions $[Y = 0.250, Z = 0.008], [Y = 0.273, Z = 0.019], [Y = 0.320, Z = 0.040]$ and $[Y = 0.390, Z = 0.070]$, initial masses from 0.15 to 20 M_{\odot} , helium-to-metal enrichment law $Y = Y_p + 2.25Z$ ($Y_p = 0.23$ is the primordial helium abundance), and both solar and ϵ -enhanced partitions of chemical elements.

In Table 1 we list the usual parameters X, Y and Z defining the initial chemical composition of a star and the corresponding $[Fe/H]$ ratio for solar-scaled and ϵ -enhanced mixtures. Columns (1) through (3) give the initial chemical composition of the adopted stellar models, whereas columns (4), (5) and (6) list the values of $[Fe/H]$ for the standard solar-scaled composition ($\epsilon = 0$), the ϵ -enhanced mixture ($\epsilon = 0.3557$) adopted by SGWC00², and another choice for an ϵ -enhanced composition ($\epsilon = 0.50$) calculated by us for the purposes of this study and to be discussed below.

Table 2 lists the detailed pattern of elements and abundance ratios adopted by SGWC00 for the solar-scaled composition ($\epsilon = 0$), the ϵ -enhanced mixtures with $\epsilon = 0.3557$, and our case with $\epsilon = 0.50$. Columns (2), (4) and (8) show the abundance A_{el} of elements in logarithmic scale ($A_{el} = \log(N_{el}/N_H) + 12$ where N_{el} is the abundance by number), columns (3), (5) and (9) display the abundance by mass X_{el} , relative to the metallicity Z , columns (6) and (10) list the element to Fe abundance ratio in spectroscopic notation, and finally columns (7) and (11)

² It is worth noticing that SGWC00 have enhanced the elements (see their Table 1 and Table 2 in this work) in such that the iron abundances for solar metallicity is equal to $[Fe/H] = 0.3557$ or equivalently $\epsilon = 0.3557$.

are the ratio $A_{\text{Fe}} = H$ which measures the degree of enhancement.

The stellar models calculated by SGW C00 for $\alpha = 0$ and $\alpha = 0.3557$ extend from the ZAMS up to either the start of the thermally pulsing asymptotic giant branch (TP-AGB) phase or carbon ignition. The major novelty of these stellar models with respect to previous calculations (Bertelli et al. 1994; Girardi et al. 1996) and TP96 is the opacity whose chemical mixture is the same of the stellar models. No details on the stellar models are given here; they can be found in SGW C00. Since it is to mention that: (i) in low mass stars passing from the tip of red giant branch (TRGB) to the HB or clump, mass loss by stellar winds is included according to the Reimers (1975) rate with $\alpha = 0.45$; (ii) the whole TP-AGB phase is included in the isochrones with ages older than 0.1 Gyr according to the algorithm of Girardi & Bertelli (1998) and Girardi et al. (2000). Because of the opacities used by SGW C00 the new tracks of high metallicity ($Z = 0.070$) do not develop the so-called hot horizontal branch (H-HB) and AGB-massive phase for low mass stars (see Reggiani & Renzini 1990; Bressan et al. 1994, for all details) thus affecting a potential source of energy in the UV and visible ranges of the spectra with some important consequences for indices like H , H_F , etc. Finally for the four sets of stellar models the corresponding isochrones and SSPs are calculated³

4. Definition of the absorption line indices for SSPs

Although the definition of the absorption line indices and how these are calculated for SSPs can be found in the original papers by Burstein et al. (1984); Faber et al. (1985); Worthey (1992); Worthey et al. (1994); Bressan et al. (1996), it may be useful to summarize here the various steps of the procedure. For the sake of easy comparison, we strictly follow the notation adopted by Maraston et al. (2003).

The definition of an absorption line index with passband λ is different according to whether it is measured in equivalent width (EW) or magnitude as given by

$$\begin{aligned} I_{\lambda} &= 1 - \frac{F_{\lambda}}{F_c} && \text{in EW} \\ I_{\lambda} &= 2.5 \log \frac{F_{\lambda}}{F_c} && \text{in Mag} \end{aligned} \quad (5)$$

where F_{λ} and F_c are the fluxes in the line and pseudo-continuum, respectively. Since the Lick system of indices (Burstein et al. 1984; Faber et al. 1985; Worthey et al. 1994) stands on a spectra library with fixed resolution of 8 Å, whereas most of the spectral libraries in use have a different resolution, the straightforward application of

³ The complete grids of stellar tracks, isochrones and SSPs are available on the web site <http://pleadi.pd.astro.it> and <http://dipastro.pd.astro.it/galadriel>.

eqs. (5) is not possible. The difficulty is with F_{λ} which depends on the spectral resolution. To overcome this problem, the so-called Best-Fitting Functions have been introduced. They express the indices measured on the observed spectra of a large number of stars with known gravity, T_{eff} , and chemical composition as functions of these parameters (Worthey et al. 1994).

Given these premises, the integrated indices of SSPs can be derived in the following way. We start from the flux in the absorption line of the generic i -th star of the SSP, $F_{\lambda;i}$

$$\begin{aligned} F_{\lambda;i} &= F_{c;i} 1 - \frac{I_{\lambda;i}}{I_{\lambda;i}} && \text{in EW} \\ F_{\lambda;i} &= F_{c;i} 10^{-0.4 I_{\lambda;i}} && \text{in Mag} \end{aligned} \quad (6)$$

where $I_{\lambda;i}$ is the index of the i -th star computed inserting in the Fitting Functions the values of T_{eff} , gravity, and chemical composition of the star, $F_{c;i}$ is the pseudo-continuum flux, and $F_{\lambda;i}$ is the flux in the passband. The flux $F_{c;i}$ is calculated by interpolating to the central wavelength of the absorption line, the fluxes in the midpoints of the red and blue pseudo-continua bracketing the line (Worthey et al. 1994).

Known the index for a single star, we weight its contribution to the integrated value on the relative number of stars of the same type. Therefore the integrated index is given by

$$\begin{aligned} I_1^{\text{SSP}} &= 1 - \frac{\frac{P}{P} \frac{F_{\lambda;i} N_i}{F_{c;i} N_i}}{\frac{P}{P} \frac{F_{\lambda;i} N_i}{F_{c;i} N_i}} && \text{in EW} \\ I_1^{\text{SSP}} &= 2.5 \log \frac{\frac{P}{P} \frac{F_{\lambda;i} N_i}{F_{c;i} N_i}}{\frac{P}{P} \frac{F_{\lambda;i} N_i}{F_{c;i} N_i}} && \text{in Mag} \end{aligned} \quad (7)$$

where N_i is the number of stars of type i -th.

When computing actual SSPs, single stars are identified to the isochrone elemental bins defined in such a way that all relevant quantities, i.e. luminosity, T_{eff} , gravity, and mass vary by small amounts. In particular, the number of stars in an isochrone bin is given by

$$N_i = \frac{Z}{m_b} (m) dm \quad (8)$$

where m_a and m_b are the minimum and maximum star mass in the bin and (m) is the mass function in number.

Indicating $F_{\lambda;i} N_i$ and $F_{c;i} N_i$ with $F_{\lambda;i}$ and $F_{c;i}$, respectively, and naming $I_{\lambda;i}$ the mean index of the isochrone bin, then eqs. (7) can be written as

$$\begin{aligned} I_1^{\text{SSP}} &= 1 - \frac{\frac{P}{P} \frac{F_{\lambda;i}}{F_{c;i}}}{\frac{P}{P} \frac{F_{\lambda;i}}{F_{c;i}}} && \text{in EW} \\ I_1^{\text{SSP}} &= 2.5 \log \frac{\frac{P}{P} \frac{F_{\lambda;i}}{F_{c;i}}}{\frac{P}{P} \frac{F_{\lambda;i}}{F_{c;i}}} && \text{in Mag} \end{aligned} \quad (9)$$

These are the equations adopted to calculate the indices of SSPs.

Table 2. Abundance ratios for the solar-scaled and α -enhanced mixtures adopted in this study. The case for $\alpha = 0.3557$ is the same as in SGW C00, the case of $\alpha = 0.50$ has been extrapolated by us (see the text for details).

Element	$\alpha = 0$:		$\alpha = 0.3557$				$\alpha = 0.50$			
	A_{el}	$X_{\text{el}}=Z$	A_{el}	$X_{\text{el}}=Z$	$A_{\text{el}}=\text{Fe}$	$A_{\text{el}}=\text{H}$	A_{el}	$X_{\text{el}}=Z$	$A_{\text{el}}=\text{Fe}$	$A_{\text{el}}=\text{H}$
O	8.870	0.482273	9.370	0.672836	0.50	+0.1442	9.570	0.770549	0.70	+0.2035
Ne	8.080	0.098668	8.370	0.084869	0.29	{0.0658	8.490	0.079983	0.41	{0.0912
Mg	7.580	0.037573	7.980	0.041639	0.40	+0.0441	8.140	0.043451	0.56	+0.0631
Si	7.550	0.040520	7.850	0.035669	0.30	{0.0558	7.970	0.033806	0.42	{0.0787
S	7.210	0.021142	7.540	0.019942	0.33	{0.0258	7.670	0.019498	0.46	{0.0352
Ca	6.360	0.003734	6.860	0.005209	0.50	+0.1441	7.060	0.005970	0.70	+0.2038
Ti	5.020	0.000211	5.650	0.000387	0.63	+0.2634	5.890	0.000495	0.87	+0.3703
Ni	6.250	0.004459	6.270	0.002056	0.02	{0.3371	6.280	0.001503	0.03	{0.4723
C	8.550	0.173285	8.550	0.076451	0.00	{0.3553	8.550	0.054828	0.00	{0.4998
N	7.970	0.053152	7.970	0.023450	0.00	{0.3553	7.970	0.016827	0.00	{0.4995
Na	6.330	0.001999	6.330	0.000882	0.00	{0.3553	6.330	0.000632	0.00	{0.5001
Cr	5.670	0.001005	5.670	0.000443	0.00	{0.3557	5.670	0.000318	0.00	{0.4997
Fe	7.500	0.071794	7.500	0.031675	0.00	{0.3557	7.500	0.022751	0.00	{0.4991

However, in order to evaluate the contribution to the total value of an index by stars of the same SSP but in different evolutionary stages, it is convenient to recast eqs. (9) in a slightly different way. With simple algebraic manipulations they become

$$\begin{aligned}
 I_1^{\text{SSP}} &= \frac{\sum_i F_{c;i} I_{1;i}}{\sum_i F_{c;i}} = \frac{X}{\sum_i f_{c;i} I_{1;i}} \quad \text{in EW} \\
 I_1^{\text{SSP}} &= 2.5 \log \frac{\sum_i F_{c;i} 10^{-0.4 I_{1;i}}}{\sum_i F_{c;i}} \quad ! \\
 &= 2.5 \log \frac{X}{\sum_i f_{c;i} 10^{-0.4 I_{1;i}}} \quad \text{in Mag}
 \end{aligned} \quad (10)$$

where $f_{c;i} = F_{c;i} / \sum_i F_{c;i}$ (or $f_{c;i} = F_{c;i} - F_{c;i}^{\text{SSP}}$) is the contribution of the stars in each isochrone bin to the total pseudo-continuum flux of the SSP. The same notation of eqs. (10) can be used to indicate the j th evolutionary phase and to evaluate the contribution of this to the building up of a generic index (see below).

5. Absorption line indices with α -enhanced: the fitting functions

The Fitting Functions are one of the most crucial issues of the whole problem because it is long known that a great deal of the final results actually depend on them. In the following we shortly summarize the most popular ones and then make our final choice.

5.1. The Worthey Fitting Functions

The widely used Fitting Functions by Worthey et al. (1994) (see also Worthey & Ottaviani 1997) depend only on T_{eff} , gravity, and $[\text{Fe}/\text{H}]$. Therefore the effect of an α -enhanced chemical composition will act only via the decrease in $[\text{Fe}/\text{H}]$ given by eq. (4) whereas the Fitting

Functions themselves will be insensitive to the abundances of the enhanced elements. Therefore, they provide only a minimum effect of an α -enhanced composition.

In contrast, many studies have emphasized that absorption line indices should also depend on the detailed pattern of chemical abundances (Barbuy 1994; Idiart & de Freitas-Pacheco 1995; Weiss et al. 1995; Borges et al. 1995). To cope with this problem two ways out are available: the empirical Fitting Functions by Borges et al. (1995) and the semi-theoretical Response Functions by Tripicco & Bell (1995).

5.2. The Borges et al. (1995) Fitting Functions

Borges et al. (1995) present empirical Fitting Functions for Mg₂ and NaD in which the effect of enhancement is considered. When this is expressed by the ratio Mg/Fe, the index Mg₂ is given by the relation

$$\ln \text{Mg}_2 = 9.037 + 5.795 \frac{5040}{T_{\text{eff}}} + 0.398 \log g + 0.389 \frac{\text{Fe}}{\text{H}} - 0.16 \frac{\text{Fe}^2}{\text{H}} + 0.981 \frac{\text{Mg}}{\text{Fe}} \quad (11)$$

It holds for effective temperatures and gravities in the ranges $3800 < T_{\text{eff}} < 6500$ K and $0.7 < \log g < 4.5$.

To make use of eq. (11), we need the value of Mg/Fe. This can be derived from the entries of Table 2. The correspondence between Mg/Fe and α can be obtained in the following way: from the pattern of abundances by Anders & Grevesse (1989), Grevesse (1991) and Grevesse & Noels (1993) we get the approximated relation

$$= 0.8 \frac{\text{Mg}}{\text{Fe}} - 0.05 \frac{\text{Mg}^2}{\text{Fe}} \quad (12)$$

According to which Mg/Fe = 0. for $\alpha = 0$ (solar-scaled abundances), and Mg/Fe = 0.43291 for $\alpha = 0.3557$. It is

worth noticing that eq. (12) yields $M_{\text{Fe/Fe}} = 1$ nearly equal to those listed in Table 2.

Unfortunately, these Fitting Functions are limited to M_{Mg_2} and M_{NaD} . For all the other indices one has to make use of the Worthey et al. (1994) Fitting Functions which are insensitive to Γ -enhanced but for the re-scaling of $[Fe/H]$. A great deal of the potential effect of enhancing the Γ -elements is lost.

5.3. The Tripicco & Bell (1995) calibration

A method designed to include the effects of enhancement on all indices at once has been suggested by Tripicco & Bell (1995, TB 95), who introduce the concept of Response Functions. These are obtained by changing one at a time the abundance of chemical elements in synthetic spectra and calculating the corresponding variations in the indices.

The authors present results for separated changes in the abundance of C, N, O, Mg, Fe, Ca, Na, Si, Cr, and Ti in steps of 0.3 dex. An additional sequence has been generated when the abundances of all the metals have been doubled (i.e. $M_{\text{Fe/Fe}} = 1.03$). The changes of the indices are calculated for three typical spectra: Cool Dwarfs ($T_{\text{eff}} = 4,575$), Turn-O stars ($T_{\text{eff}} = 6,200$), and Cool Giants ($T_{\text{eff}} = 4,255$) stars. They constitute the milestones of the calibration. Finally they apply their Response Functions to correct the Worthey et al. (1994) indices.

The correcting technique is expressed by the relation (see TFW G 00):

$$I = \frac{I}{I_0} = \sum_i \frac{Y_i}{Y} [1 + R_{0.3}(X_i)]^{(X_i - H_i) / 0.3} \quad (13)$$

where $R_{0.3}(X_i)$ is the Response Function for element i at $X_i = H_i + 0.3$ dex. This is given by $(R_i)_0$ where R_i is the value for each element in unit of standard errors σ_0 as tabulated in TB 95. Using this equation one makes an iterative correction to the initial value of the index that depends on the number of enhanced elements. This means that increasing the abundance of a single chemical element, the effect of it is propagated to the whole spectrum. Furthermore, this equation assumes that the percent change is constant for each step of 0.3 dex.

However, as emphasized by TFW G 00, eq. (13) above, while securing that the indices tend to zero for small abundances, lets them to increase with the exponent $X_i - H_i = 0.3$. For abundances higher than $X_i - H_i = +0.6$ dex, the exponent may become too large and consequently the correction may diverge.

To apply eq. (13), one has to fix the abundance of those elements that are enhanced with respect to the solar partition. With the abundances specified in Tables 1 and 2 we calculate the corrections to be applied to each index of the Worthey et al. (1994) system for the milestones of the TB 95 calibration. The results are summarized in Table 3

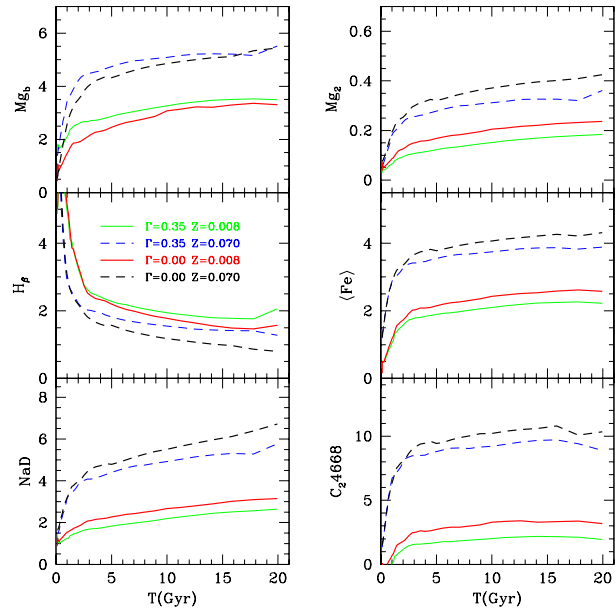


Fig. 1. Evolution of six indices (M_{Mg_b} , M_{Mg_2} , H , h_{Fei} , N_{NaD} and C_24668) as function of the age. The heavy lines show the indices for solar-scaled partition of elements ($\Gamma = 0.0$), whereas the thin lines show the same but for the partition of Γ -enhanced of SGW C 00 ($\Gamma = 0.3557$). Only two metallicities are displayed for the sake of clarity, i.e. $Z = 0.008$ (solid lines) and $Z = 0.07$ (dashed lines).

for $\Gamma = 0.3557$ and $Z = 0.07$. They will be used to correct the partial indices along isochrones and SSPs according to the standard spectral synthesis technique (e.g. Bressan et al. 1994; Charlot & Bruzual 1991)

In concluding this section it is worth reminding the reader that Thomasson et al. (2003) have derived a different formulation of the correction factor given by the eq. (13) above, which however yields similar results provided that $R_{0.3}(X_i) \ll 1$. See Thomasson et al. (2003) for all details.

6. Building the indices of SSPs

In this study we will make use only of the TB 95 calibration both for the sake of brevity and because we intend to compare our results with those by TFW G 00 who adopted the same transformation.⁴

With the aid of the SGW C 00 SSPs, the pattern of abundances and abundance ratios presented in Tables 1 and 2, and the TB 95 calibrations and its companion corrections listed in Table 3, we finally derive the whole set of indices on the Lick System for SSPs of different age, metallicity and Γ . To apply the TB 95 corrections we proceed as follows: for each elemental bin of an isochrone and/or SSP with assigned Γ , we derive the index according to the fitting functions and correct it according to

⁴ Extensive tabulations of indices based on the Worthey et al. (1994) and Borges et al. (1995) Fitting Functions are available from the authors upon request.

Table 3. Corrections to the indices of the milestone stars of the TB 95 calibration for the enhanced mixtures adopted in this study.

	= 0.3557			= 0.50		
	Cool Dwarf	Cool Giants	Tum-O	Cool Dwarf	Cool Giants	Tum-O
1 C N ₁	{0.86924	{0.72020	0.06469	{0.94293	{0.83312	0.09187
2 C N ₂	{0.71071	{0.64423	0.12762	{0.82519	{0.76609	0.18368
3 C a4227	0.49210	1.16835	0.29614	0.75595	1.97106	0.44172
4 G 4300	{0.22074	{0.22678	{0.22147	{0.29578	{0.30336	{0.29654
5 F e4383	{0.30427	{0.23921	{0.38539	{0.39919	{0.31887	{0.49505
6 C a4455	0.10268	0.21882	{0.16268	0.14711	0.32019	{0.22078
7 F e4531	{0.10913	0.00080	{0.08902	0.15680	0.00138	{0.12246
8 C ₂ 4668	{0.86564	{0.74347	{0.75727	{0.94037	{0.85224	{0.86310
9 H	3.65512	0.00000	0.02004	7.72597	0.00000	0.02826
10 F e5015	{0.01921	{0.03958	{0.00743	{0.02825	{0.05526	{0.01037
11 M g ₁	{0.06069	{0.40588	{0.40464	{0.08364	{0.51863	{0.51721
12 M g ₂	0.01182	{0.00694	{0.00749	0.01711	{0.00923	{0.00959
13 M g ₃	0.17311	0.89905	0.32837	0.25210	1.46399	0.49168
14 F e5270	{0.13721	{0.21170	{0.09744	{0.18695	{0.28398	{0.13329
15 F e5335	{0.19050	{0.11207	{0.27049	{0.25670	{0.15351	{0.35755
16 F e5406	{0.21400	{0.21041	{0.41880	{0.28684	{0.28226	{0.53294
17 F e5709	0.06876	0.15365	{0.15397	0.09839	0.22265	{0.20837
18 F e5782	{0.22121	{0.17053	{0.60409	{0.29618	{0.23099	{0.72772
19 N aD	{0.19018	{0.29959	{0.50848	{0.25680	{0.39390	{0.63116
20 T iO ₁	0.00000	{0.76939	0.04056	0.00000	{0.87285	0.05485
21 T iO ₂	{0.33876	{0.56007	{0.27143	{0.44076	{0.68448	{0.35868

eq. (13) by interpolating the entries of Table 3 as appropriate to the current values of T_{eff} , and gravity (luminosity class), and follow the whole procedure described in Section 4. Extensive tabulations of the complete set of the Lick System for SSPs of different age, metallicity ($Z = 0.008, 0.019, 0.040$, and 0.070) and $(0, 0.35$ and $0.5)$ are available from the authors. The layout of the data is presented in the description of Table A.1 given in the Appendix A (these are also available on the web site <http://dipastro.pd.astro.it/galadriel>).

To illustrate the results we show in Fig. 1 the temporal evolution of six important indices, i.e. $M_{\text{g}_1}, M_{\text{g}_2}, H, \text{hFei}, \text{NaD}$ and C_24668 , for the following combinations of metallicity and Z , namely $Z = 0.008$ (solid lines) and $Z = 0.070$ (broken lines), $= 0$ (heavy lines) and $= 0.3557$ (light lines). The age goes from 0.01 G yr to 20 G yr .

The merit of this set of indices is the internal consistency as far the chemical parameters are concerned. The stellar models and the indices have been calculated with the same pattern of abundances.

All indices show the same behavior. For ages older than about 3 G yr they all tend to attenuate (age-degeneracy). In order to quantify the response of the indices to changes in metallicity Z , enhancement factor ϵ , and age T we calculated the relative per cent variations

$$\frac{I}{I_{z;T}} \quad \text{and} \quad \frac{I}{I_{T;z}}$$

where I stands for the generic index, and the variations I are calculated for $Z = 0.070$ ($0.008 = 0.062$, $T = 15$

$= 10 \text{ G yr}$, and $= 0.35$ ($0 = 0.35$). The per cent variations are evaluated at fixed values of metallicity ($Z = 0.008$ and $Z = 0.70$), enhancement factor ($\epsilon = 0$ and 0.35), and age ($T = 5, 10$ and 15 G yr) as appropriate. The results are summarized in Table 4 for the six indices shown in Fig. 1. These evaluations can be easily extended to any index of the Worthey et al. (1994) list. It is soon clear that C_24668 and NaD strongly depend on metallicity and to a lesser extent on Z , whereas they scarcely depend on the age. All remaining indices almost evenly depend on the three parameters with little resolving power.

In order to clarify the role played by each evolutionary phase of the SSPs in the building process of the indices we apply the eqs. (10) to each phase

$$I^{\text{SSP}} = \sum_j f_{c;j} I_j \quad \text{in EW}$$

$$I^{\text{SSP}} = 2.5 \log \epsilon \sum_j f_{c;j} 10^{0.4 I_j A} \quad \text{in mag} \quad (14)$$

where the index j stands for the generic phase, I_j is the integrated index of the phase, $f_{c;j} = \sum_i f_{c;i}$ is the fraction of the pseudo-continuum flux of the phase with respect to the total, and i denotes the generic star belonging to the phase. To this aim the SSPs have been split into five evolutionary phases, i.e. (1) up to the main sequence turn-off (TO), (2) from the TO to the tip of the RGB (T-RGB), (3) from this to the end of core He-burning (HeB), (4) from this stage to the end of the TP-AGB, and finally (5) from this latter down to the formation of Planetary Nebulae

Table 4. Relative per cent variations of the indices at changing age, metallicity, and . The indices are for the SSPs of SGW C 00.

T (G yr)	Z	H	M g _b	M g ₂	hFei	NaD	C ₂₄₆₆₈
5.00	0.06	0.00	{29 %	76 %	91 %	76 %	111 %
10.00	0.06	0.00	{34 %	58 %	81 %	68 %	107 %
15.00	0.06	0.00	{35 %	57 %	77 %	65 %	104 %
5.00	0.06	0.35	{20 %	65 %	128 %	88 %	141 %
10.00	0.06	0.35	{20 %	56 %	105 %	78 %	125 %
15.00	0.06	0.35	{20 %	49 %	89 %	73 %	113 %
T (G yr)	Z	H	M g _b	M g ₂	hFei	NaD	C ₂₄₆₆₈
5.00	0.008	0.35	4 %	17 %	{38 %	{12 %	{19 %
10.00	0.008	0.35	9 %	6 %	{26 %	{13 %	{18 %
15.00	0.008	0.35	18 %	7 %	{23 %	{13 %	{16 %
5.00	0.070	0.35	16 %	10 %	{13 %	{6 %	{8 %
10.00	0.070	0.35	31 %	5 %	{16 %	{8 %	{11 %
15.00	0.070	0.35	43 %	2 %	{18 %	{9 %	{13 %
T (G yr)	Z	H	M g _b	M g ₂	hFei	NaD	C ₂₄₆₆₈
10.00	0.008	0.00	{31 %	33 %	34 %	19 %	30 %
10.00	0.070	0.00	{37 %	18 %	24 %	12 %	26 %
10.00	0.008	0.35	{21 %	21 %	41 %	18 %	35 %
10.00	0.070	0.35	{22 %	10 %	17 %	9 %	20 %

and incipient White Dwarf cooling sequence (P-AGB)⁵. In Fig. 2 we show the building up a few selected indices for a typical SSP of solar com position (no enhancement in -elements) and age of 15 G yr. Similar results are obtained for other choices of the chemical parameters and ages. As expected the largest contribution to an index comes from phases (1) and (2), with a minor contribution from phase (3). All the rest is negligible. We will examine this point in more detail below. The results presented in Fig. 2 are virtually identical to those in Fig. 2 of Maraston et al. (2003).

7. Deriving ages, metalicities and abundance ratios from absorption line indices

7.1. Which indices to choose?

As already mentioned above, the ultimate scope of a system of indices is to derive the age, metallicity, and enhancement factor of the stars in aggregates of different complexity going from clusters to galaxies, the EGs in particular. To proceed further in the analysis one has to find three or more indices, or combination of these, most sensitive to the parameters in question. It is commonly thought that indices like H are good age indicators, whereas others like M g_b, hFei, M g₂ are good metallicity indicators. However, the results presented in the previous sections and the discussion below will clarify that a certain degree of degeneracy among the different parameters is always present so that there is no clear one to one dependence of an index from age, metallicity and degree of enhancement.

Furthermore, the choice is often dictated by the available data-bases of indices. Among others, the most pop-

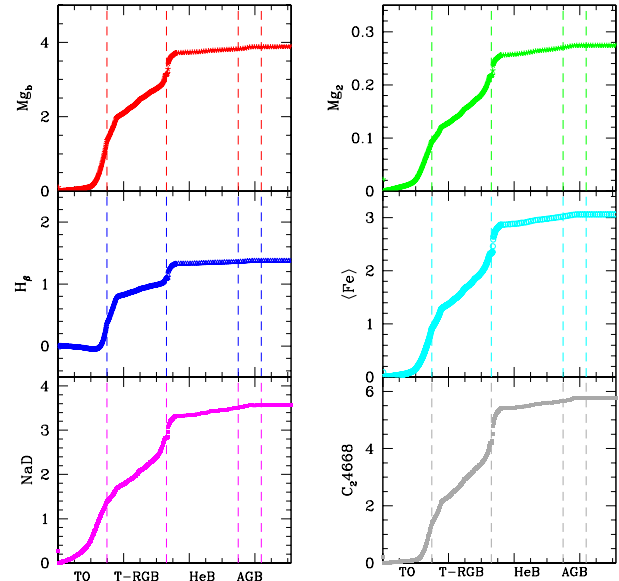


Fig. 2. Building up of a few selected indices for a SSP with solar com position, no enhancement in -elements (Z=0) during the 5 evolutionary phases into which the SSP has been split up. The abscissa indicates the evolutionary phases, whose last stage is marked by the vertical lines. It is worth remind the reader that for the sake of clarity the phase spacing has been arbitrarily changed with respect to the underlying phase duration. The ordinate is the running value of the index. The different steps show the varying contribution of each phase. By definition the SSP index corresponds only to the final value.

⁵ To be precise this classification strictly applies to SSPs older than say 0.1 Gyr, i.e. those whose TO mass is smaller than about 5 M_{sun}.

ular data-bases are the catalogs by Gonzalez (1993) for nearby old early-type galaxies, and the Trager "IDS Pristine" sample (see Trager 1997, Table 3.1) for the central regions of elliptical galaxies.

For the purposes of the present study, the analysis will be limited to these samples of data, leaving aside for the time being other more recent compilations.

The González (1993) catalog provides H , the iron-group indices, and the Mg-group indices for the region within the radius $R_e = 8$ for a sample of nearby old galaxies.

The Trager (1997) sample lists H , the higher-order Balmer line indices ($H_A, H_{\beta}, H_F, H_{\gamma}$), the iron-peak indices, C_24668 , and others.

We adopt here the indices H , $hFei$, Mg_b , Mg_{β} , NaD and C_24668 on which much work has been done in the past so that the comparison is possible.

7.2. The Minimum-Distance method

As already proposed by TFWG00 the so-called Minimum-Distance M method is perhaps best suited to our purposes. Suppose that a galaxy and/or a star cluster is characterized by a set of observationally measured indices $I_{i,obs}$, from which we want to infer the age, the metallicity Z , and the degree of enhancement ϵ . On the theoretical side, suppose we have the corresponding indices tabulated as a function of the same quantities in form of discrete grids of values $I_{i,th}(t_j; Z_k; \epsilon_l)$ where j, k , and l vary from 1 to a certain value as appropriate. In the space of the indices I_i we define the distance between the observational set $I_{i,obs}$ and a generic point of the correspondent space $I_{i,th}$:

$$D = \left(\sum_i (I_{i,th} - I_{i,obs})^2 \right)^{0.5} \quad (15)$$

By varying $I_{i,th}$ over the whole grid space we find the particular triplet j, k, l for which D is minimal. This means to fix the age, metallicity Z , and ϵ .

In the case of the star clusters, the above method is quite safe because the age, metallicity and ϵ of the stars in a cluster are confined within narrow ranges of values, so that a cluster is well-mimicked by a SSP. In real galaxies, the situation is more complicated and risky because even in the case of EGS a mix of stellar populations with different age and chemical properties is likely to exist. Therefore the approximation to SSP is no longer valid and SSPs should be replaced by galactic models incorporating the history of star formation and chemical enrichment and the indices to be used should take into account the contribution from all stellar components. Integrated indices for model galaxies have been calculated by Tantalo et al. (1998b) but never applied to this kind of analysis. Therefore, since most if not all of the studies in literature are based on the SSP approximation, we will adopt it also here.

To be applied the Minimum-Distance M method requires large grids of SSPs with fine spacing in age, metallicity and ϵ . The SGWC00 grids of SSPs cover a wide age range with narrow spacing, and span a large range in metallicity, $0.008 \leq Z \leq 0.070$. Thanks to their regular behavior over large ranges of age and metallicity additional SSPs can

be added by interpolation. However, the grids are only for $\epsilon = 0$ and $\epsilon = 0.3557$. The simple extrapolation to higher values of ϵ may be risky, because of the non linear response of the calibration to variations of this important parameter. To cope with this problem without embarking in the tedious and time consuming calculations of new grids of stellar models with higher degree of enhancement, the following strategy has been adopted. The detailed stellar models calculations by SGWC00 have shown that keeping constant all other physical parameters passing from $\epsilon = 0$ to $\epsilon = 0.3557$ or equivalently re-scaling $[Fe/H]$ as appropriate, the stellar models by themselves do not change in a dramatic fashion but for expected effects due to the lower $[Fe/H]$ and the higher $[Mg/H]$ that can be easily handled. Taking advantage of it, first we prepare a new pattern of chemical abundances having $Z = 0.50$ by extrapolating the variations in individual species passing from $Z = 0$ to $Z = 0.3557$ according to the recipe by SGWC00. These have already been shown in Tables 1 and 2. Second, using the SSPs by SGWC00 we calculate new grids of indices with the new pattern of abundances for $Z = 0.50$. Finally, we generate the large grid of SSPs suited to the Minimum-Distance M method. The grids span the ranges

$$\begin{array}{llll} 0 & T \text{ (Gyr)} & 20 \\ 0.008 & Z & 0.070 & \text{or} \\ 0: & 0.50 & & \end{array} \quad [Z=H] \quad 0.68$$

The age spacing is the same as in the SGWC00 data-base of isochrones. For the metallicity, by adopting $Z = 0.019$ $X = 0.708$, we replace the abundance by mass Z with $[Z/H]$ so that the results can be immediately compared to those by TFWG00. The spacing in metallicity is $[Z=H] = 0.022$. Finally, ϵ is spaced by $\epsilon = 0.01$.

7.3. Analysis of the González sample

Using the above grid of indices, we analyze the same sample of the González (1993) catalog of EGSs studied by TFWG00 and compare the results. The indices we have considered are H , Mg_b and $hFei$. The observational data for the indices and the solutions for age, metallicity and degree of enhancement are listed in Table B.1 given in the Appendix B.

Fig. 3 compares the results we obtain here (upper panel) with those derived by TFWG00 for their $C^{18}O^{+}$ model (bottom panel), more details on this model are given below. The various histograms show the fraction of galaxies N_{Gal}/N_{Tot} as a function of the age in Gyr (left panel), the metallicity $[Z=H]$ (middle panels) and the enhancement factor ϵ (right panels). Since the observational indices are affected by some uncertainty, i.e. H (H_A), Mg_b (Mg_{β}) and $hFei$ ($hFei$), we derive the uncertainty associated to

⁶ See Section 8.3.2 for the correspondence between our definition of ϵ and that of $[Mg/H] = [Mg/H]_{Fe}$ given by TFWG00.

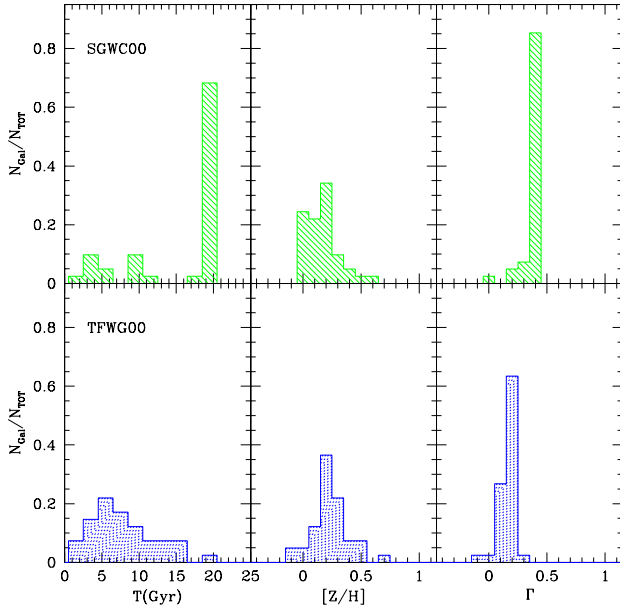


Fig. 3. Distribution histograms of the age T (in G yr), metallicity ($[Z/H]$), and enhancement factor (from left to right) for the galaxies in the Gonzalez's Sample with $R_e = 8$ -aperture. The results are obtained applying the Minimum-Distance Method to the index-triplet H , M_{gb} , $hFei$. The top panel is for the SGW C00 model, whereas the bottom panel is for the CO^+ -model of TFW G00, shown here for comparison⁶.

the theoretical determinations by searching the grid at $[H]$ (H), M_{gb} , $hFei$, $[H]$, M_{gb} (M_{gb}), $hFei$, and $[H]$, M_{gb} , $hFei$ ($hFei$) and taking the maximum deviations, $\max(T)$, $\max([Z/H])$, and $\max(\Gamma)$ as the associated uncertainties. The results are given in Table B.1 and displayed in Fig. 4, which clearly shows that the observational uncertainty on the indices scarcely affects the determinations of the age, metallicity, and Γ but for a few exceptions. Thanks to it, we will not carry out the analysis of the uncertainty brought about by the observational errors unless otherwise specified.

Even considering the uncertainty due to the observational "errors", there are important differences between TFW G00's results and ours, in particular as far as the age is concerned. While in TFW G00 the majority of galaxies have ages in the range 1 to 15 G yr with a peak at about 6 G yr, in our analysis the majority of galaxies turn out to be very old (the formal age is 20 G yr which simply is the maximum age in our data base). There seems to be a gap at about 16 G yr separating the very old galaxies from the younger ones (age less than 15 G yr). These latter in turn seem to split in two sub-groups separated by a gap centered at about 7.5 G yr. On the other hand, the metallicity and distribution are not too different, even if our metallicity seems to be preferentially lower than in TFW G00, whereas the opposite occurs for Γ which in general is 0.2 dex higher than in TFW G00 and nearly constant. There is a final remark worth being made here on

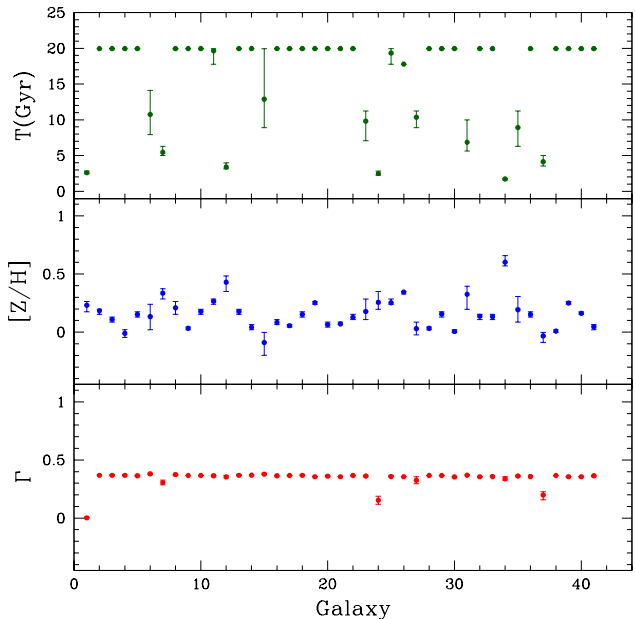


Fig. 4. Analysis of the effects due to uncertainty affecting the observational indices limited to the results presented in the top panel of Fig. 3. The vertical bars show the range spanned by the age, metallicity and assigned to each galaxy of the Gonzalez (1993) list due to the uncertainty affecting the observational data. The x-axis is the identification number of the galaxies in the catalog. The top panel is the age T , the mid panel is the metallicity $[Z/H]$, and the bottom panel is the enhancement factor Γ .

the apparent contradiction between the M_{gb} vs. the velocity dispersion shown by the observational data (Bender et al. 1996; Ziegler & Bender 1997) and the nearly constant value of Γ we have found. Since the Minimum-Distance Method requires that the observational values of the indices of a given galaxies are reproduced (see for instance the control check made in Section 9 below), this would imply that the correlation M_{gb} vs. Γ is also matched (no use is made here of the parameter Γ). This simply means that passing from indices to abundance ratios is not as straightforward as it may look.

The major difficulty of the above results is with the age, because too many galaxies have the formal age of 20 G yr, which on one hand is unacceptably too old on the other hand is the maximum value of the age grid. This simply means that the solution is poorly determined and all these cases should be discarded. Arbitrarily dropping all cases for which the age is older than 15 G yr we are left with a handful of galaxies, whose ages fall in the range 3 to 15 G yr.

Thomas & Maraston (2003) have argued that since SGW C00 enhanced stellar tracks are bluer than the standard ones, they yield higher H and weaker metallicity line and weaker indices like M_{gb} , M_{gb} , $hFei$ etc. Based on this, Thomas et al. (2003, TM03) have concluded that

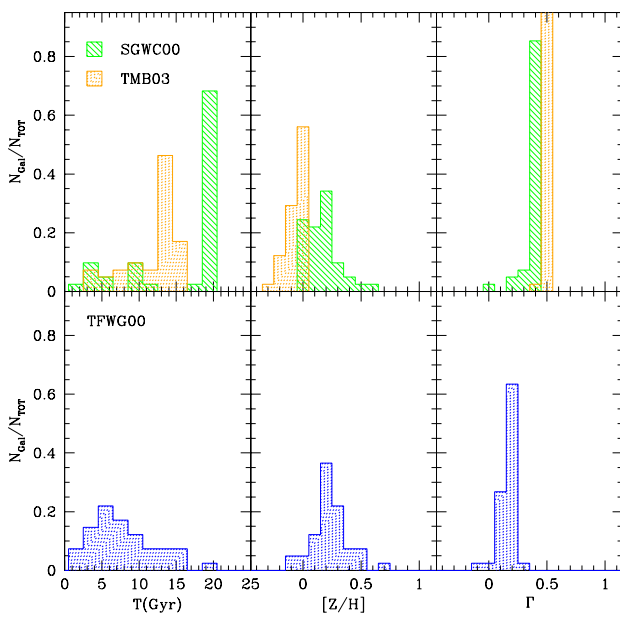


Fig. 5. Distribution histograms of the age T (in G yr), metallicity ($[Z/H]$), and enhancement factor (from left to right) for the galaxies in the González's Sample with $R_e = 8$ -aperture. The results are obtained applying the Minimum Distance Method to the index triplet H , Mg_b , $hFei$. The top panel is for the SGWC00 and the Thomas et al. (2003) models, whereas the bottom panel is for the C^{0+} -model of TFWG00, shown here for comparison.

the SWGC00 tracks lead to extremely high ages, without strong impact on metallicity and enhancement factor.

Even though we agree on the remark that enhanced stellar models tend to give ages older than the one derived from standard models, the real point of difficulty is that the age spread found by TFWG00 (with very few objects older than 15 G yr and the vast majority in the range 3 to 10 G yr) is not recovered. Interestingly enough the same result is also obtained using the Thomas & Maraston (2003) grids of theoretical indices. This is shown in Fig. 5 where the González (1993) sample is re-analyzed using the theoretical indices by Thomas & Maraston (2003). Once again the majority of galaxies turn out to be older than 10 G yr, more than 50% are indeed in the age 13–16 G yr; incidentally 15 G yr is the age limit of the Thomas & Maraston (2003) grids. As far as the degree of enhancement and metallicity are concerned, the distribution of peaks in both cases at $r \approx 0.4$ –0.5, whereas the distribution of metallicities is shifted to lower values by about 0.3. In any case Thomas & Maraston (2003) SSPs yield ages that are close to those presented here and much different from the ones derived by TFWG00.

Therefore, different stellar models and different chemical compositions are not the sole cause of the embarrassing disagreement between TFWG00 and the present results (inclusive of the ones derived from the Thomas & Maraston (2003) grids). We suspect that reality is more

complex than this comes from the high number of galaxies for which the formal solution is an age at the limit of the grids. It is therefore mandatory to examine the whole problem starting from its fundamentals.

8. Why such big differences?

There are several possible causes for the large difference between the TFWG00 determinations of age, metallicity and ours: stellar models and SSPs in use, pattern of abundances in the enhanced mixtures, and details on the construction of the indices grids and their extensions to regions of the parameter space not covered by the original models. In the following we intend to discuss separately the above topics with the aid of suitable experiments.

8.1. Recovering the TFWG00 solution

We start the analysis with a brief overview of the procedure followed by TFWG00 to derive ages, metallicities and degree of enhancement. First they adopt the SSPs by Worthey (1994), which have essentially solar abundance ratios, second they define a suitable scheme to derive non solar compositions, third they make use of the TB95 response functions to derive for the generic index the correction $I = I/I_0$, see eq. (13) above and the entries of their Table 5, to pass from solar to enhanced compositions, and finally they extend the original grids of SSPs (by means of linear interpolations and extrapolations) to get new grids suited to the Minimum Distance Method. Strictly repeating the various steps above, their solution is immediately recovered. For the sake of illustration we show in Fig. 6 the solution we derive for their C^{0+} model (however no extrapolation of the grids beyond the original ranges of ages and r has been applied for the sake of brevity). The top panel shows how the situation would be if only solar scaled SSPs are adopted. The results in the bottom panel, which allow for changes in the enhancement factor, are virtually identical to those in their Fig. 7. This is necessary check to reassure ourselves that we are correctly interpreting their results.

8.2. The stellar models-isochrones-SSPs

As already mentioned, the indices of TFWG00 are based on the SSPs calculated by Worthey (1994). These latter in turn are obtained by patching together stellar models (isochrones) by Vandenberg (1985); Vandenberg & Bell (1985); Vandenberg & Laskarides (1987), and the Revised Yale Isochrones (Green et al. 1987, RYI). The Vandenberg isochrones have been extended up to the T-RGB phase using the giant branches of RYI with a number of extrapolations. As far as later stages are concerned, namely HB and AGB, they have been added by means of the Fuel Consumption Theorem of Buzzoni (1989). See Worthey (1992) and Worthey (1994) for all details. The least we can remark is that these SSPs are a patchwork of many sources of data, which may not be fully self-consistent in

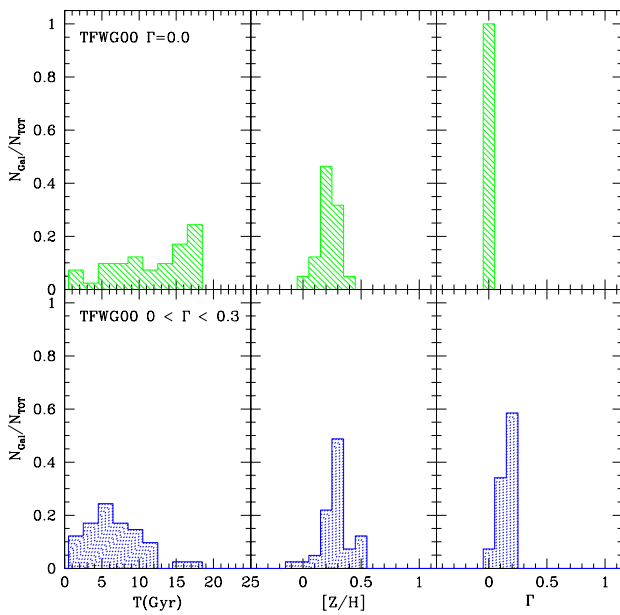


Fig. 6. Distribution histograms of the age T (in G yr), metallicity ($[Z/H]$), and enhancement factor (from left to right) for the galaxies in the Gonzalez's Sample with $R_e = 8$ -aperture. The results are obtained applying the Minimum Distance Method to the index-triplet H , M_{gb} , $hFei$ for Worthey (1994) SSPs with the sole solar mixture (top panel) and the same SSPs but with both solar and enhanced mixture of the TFWG00 C^0O^+ -model (bottom panel). These latter results are virtually identical to those of Fig. 7 in TFWG00.

all details. It is hard, if not impossible, to trace back all aspects of internal inconsistency (different physical input in the underlying stellar models, such as opacity, equation of state, mixing length parameter etc., initial chemical composition, important details of short lived phases, and finally numerical accuracy).

In contrast, the SSPs of SGW C00 stem from accurate evolutionary stellar models and isochrones, homogeneous in their input physics and extending up to the latest visible phases. Their net advantage is (at least) the internal consistency, which secures that no spurious effects are added to the problem. Only SSPs of the same quality as those of the Padova Library ought to be adopted.

Given these premises, it might be worth of interest (i) to assess the contribution from stars in different evolutionary phases to the total value of the SSP indices; (ii) to estimate the uncertainty in the index values caused by neglecting late evolutionary phases; (iii) to compare the TFWG00 SSPs with the closest SSPs of the Padova library; (iv) to examine in some detail the effect of core HeB and later phases at old ages and/or very high metallicities; (v) to compare results for the same type of SSPs but different metallicities and enhancement elements; (vi) finally, to mention at least the effect of the enrichment law $Y = Z$.

(i) Relative contribution by different phases. To this aim, we have split the SSPs into the same number of evolutionary phases already used in Section 6 and considered the SSPs by TP 96 with solar metallicity and no enhancement in α -elements ($r = 0$). Although these SSPs are somewhat different from the corresponding ones by SGW C00, they offer the advantage that the various evolutionary phases have already been marked by the authors.

In Fig. 7 we show the relative contribution of each phase as function of the SSP age. The relative contribution is defined as follows

$$\frac{I_j}{I_{\text{SSP}}} = \frac{I_j - I_{j-1}}{I_{\text{SSP}}} \quad (16)$$

where I stands for the generic index, j for the phase running from 1 to 5 ($j-1=0$ is the main sequence), I_{SSP} for the total, and finally the phase contribution I_j is calculated according to eq. (14).

On the average, lumping together the various steps in three major contributions and neglecting details depending on the particular index under considerations, we find $I_{\text{TO}} = I_{\text{MS}} = 0.1$, $I_{\text{TRGB}} = I_{\text{TO}} = 0.3 - 0.5$, $I_{\text{AGB+PAGB}} = I_{\text{TRGB}} = 0.1$.

(ii) Neglecting late evolutionary phases. Since not all SSPs in literature contain all evolutionary phases predicted by stellar evolution theory (in some extreme cases they do not extend beyond the TO or the TRGB) it is worth looking at the uncertainty introduced in the calculation of indices by neglecting late evolutionary phases. To this aim we have calculated the indices of fictitious SSPs whose last evolutionary phase is the TO, the TRGB, the end of core HeB, the end of the TP-AGB, and the P-AGB. Once again, the SSPs in use are those by TP 96. Before discussing the results we would like to emphasize the profound difference between this experiment and the analysis of the contribution by different evolutionary phases to the total index we have presented above. Now each truncated SSP is complete, no other evolutionary phase exists beyond the considered truncation stage. The resulting index is physically consistent even though it does not correspond to a real value.

The results of this experiment are shown in Fig. 8 which displays the difference

$$I = I^{\text{Phase}} - I^{\text{TO}} \quad (17)$$

For the sake of simplicity we display only the quantities $I = I^{\text{TRGB}} - I^{\text{TO}}$ and $I = I^{\text{HeB}} - I^{\text{TO}}$.

The experiment immediately clarifies what follows: (a) the RGB and HeB stages may significantly affect the total index as already known from the analysis of the relative contributions; (b) depending on the age and index under examination the Post-TO phases may either increase or decrease the index expected from the sole stars up to the TO. When the difference is positive, neglecting stages beyond the TO and/or the TRGB means that the index in question is underestimated (often by a significant amount). The opposite when the difference is negative. (c)

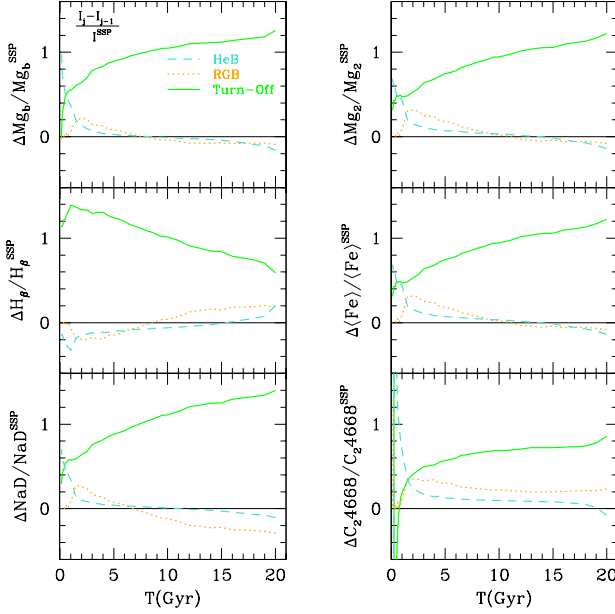


Fig. 7. The relative contribution to an index by each phase as function of the age (in G yr). The SSPs are those by TP 96 with $Z = 0.02$ and $\alpha = 0$. The Solid, dotted and dashed lines show the contribution from TO, T-RGB, and HeB phases respectively. See the text for more details.

In any case all phases beyond core HeB do not significantly contribute to the final value of an index.

Chief conclusion of the above analysis is that detailed and accurate calculations of SSPs throughout all evolutionary phases are the main prerequisite to obtain reliable indices. Passing to the SGW C00 library of SSPs, we recover most of the trends presented above, even if there are significant differences in the details.

(iii) Which of the Padova SSPs get closer to TFW G00? Going back to the SSPs adopted by TFW G00, they are not strictly equivalent to those in usage here first because they are for solar-scaled compositions and second they stand on stellar models calculated with somewhat older physical input. To cope with the latter point of inconsistency, we prefer to compare the SSPs of Worthey et al. (1994) with those of TP 96 as they have been calculated with a physical input (opacity, equation of state, nuclear reaction rates etc.) more or less coeval to that adopted for the SSPs by Worthey et al. (1994). It is worth recalling that both libraries, even if in a different fashion, include all stellar evolutionary phases.

In Fig. 9 we compare the indices calculated with the TP 96 SSPs including all evolutionary phases (thin lines) with those of Worthey (1994) models (full dots and lines). Even in this case the differences among the two grids are very large. We also compare TP 96 SSPs limited to the T-RGB (heavy lines). Remarkably, the Worthey et al. (1994) grid supposedly extending up to the latest evolutionary phases is actually in closer agreement with the TP 96 truncated at the T-RGB. This suggests that part of

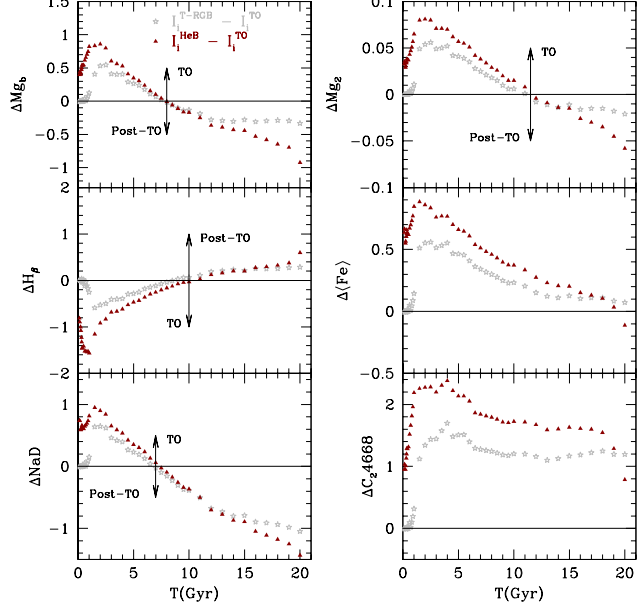


Fig. 8. Indices from truncated SSPs, whose last evolutionary stage is the TO, the T-RGB, and the end of the HeB, as function of the age T in G yr. The displayed quantities are the differences $I = I^{\text{T-RGB}} - I^{\text{TO}}$ (empty stars) and $I = I^{\text{HeB}} - I^{\text{TO}}$ (filled circles). The SSPs are those by TP 96 isochrones with $Z = 0.02$ and $\alpha = 0$.

the disagreement could reside in the way the HeB stages are included by Worthey et al. (1994).

(iv) Effect of core HeB and later phases. Comparing the complete SSPs of TP 96 with those by SGW C00, see Fig. 1, we note the important effect on the indices caused by core HeB stars at varying age and metallicity. In brief, at normal metalicities, say up to $Z \leq 0.008$, a sort of upper limit for stars in Globular Clusters, at very old ages (older than about 15 G yr) the indices suddenly increase (H) or decrease (e.g. Mg_2 , Mg_b , hFe). The same occurs for metalicities greater than $Z \geq 0.008$, but the age at which the trend is reversed gets lower and lower at increasing metallicity. The reversal of the indices at old ages and/or high metalicities is fully explained by the behavior of core HeB stars. Limiting the discussion to low mass stars and old ages in turn, the rule is that core HeB (or HB morphology) takes place closer and closer to the Hayashi line at decreasing age and/or increasing metal content. The trend is the result of three concurring effects: the value of the TO mass (age), the amount of mass lost at the T-RGB (details of the adopted mass-loss rate are very important in this context), and the metallicity itself. Under current estimates for the efficiency of mass-loss, the HB phase gets redder and redder at increasing metal content and the AGB phase takes place along the Hayashi line (see Chiosi et al. 1992, for all details). This is the typical behavior of stars in Globular Clusters. However, as pointed out long ago by Brocato et al. (1990); Castellani & Tomabene (1991); Hord et al. (1992); Domman et al.

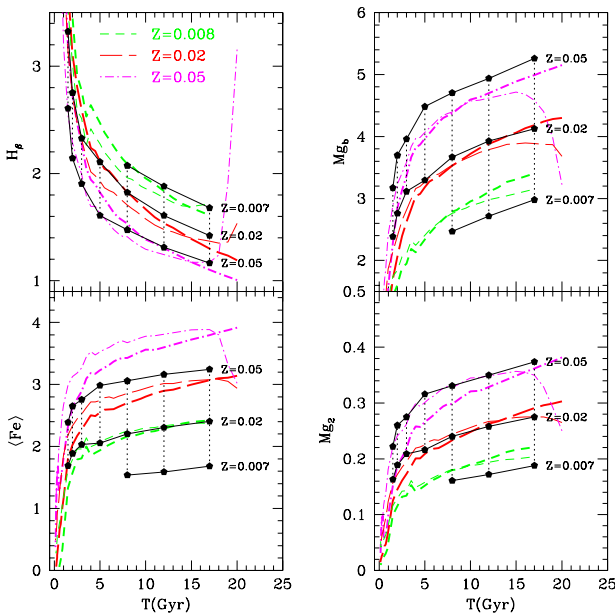


Fig. 9. Comparison of four selected indices calculated with different SSPs and abundance patterns. All the indices are plotted as functions of the age in G yr and for different metallicities as indicated. The thin lines are the indices calculated with the TP 96 SSPs including all evolutionary phases. The thick lines are the same but for SSPs limited to the T-RGB phase. The metallicities are $Z = 0.008, 0.02$, and 0.05 (dashed, long-dashed and dot-dashed respectively). The full circles joined by thin solid and dotted lines are the indices of the Worthey (1994) grid for metallicity $Z = 0.007, 0.02$, and 0.05 as indicated.

(1993); Fagotto et al. (1994), and Bressan et al. (1994), if the metallicity happens to be higher than the typical value for the most metal-rich globular clusters, this simple scheme breaks down. In brief at high metallicity (close to the solar value), the evolution does not proceed toward and along the AGB, but toward a slow phase taking place at high effective temperature without going back toward the AGB (the so-called AGB-manque phase, see Greggio & Renzini 1990, for more details). For solar and twice solar metallicity, the blue phase begins during the shell He-burning. For 3 times solar metallicity it begins during the late stages of core He-burning. For still higher metallicity a large fraction of the core He-burning lifetime is spent at very high effective temperature and high luminosity, see Bressan et al. (1994) for more details. All this would immediately reflect onto the broad-band colors and indices that are sensitive to the flux emitted in UV-visible part of the spectrum. The effect is that many indices reverse their trend at increasing age and increasing metallicity as already shown in Fig. 9 for the indices H_{α} , Mg_2 , Mg_b , and $hFei$. The SSPs by SGW C00 do not display the above trend (at least in range of ages and metallicities they have considered) because of the different physical of the stellar models, in particular the mixing length, the opacity, and

the prescription for mass-loss during the RGB and AGB phases (see SGW C00 for details).

(v) Varying metallicity and Z . Although this topic has already been addressed in Section 6 and partially shown in Fig. 1, it is worth of interest to stress here once more how the indices, based on the same type of stellar models, depend Z and considering the all range of values spanned by the parameters. The SSPs are those by SGW C00. The results are shown in Fig. 10 as function of the age and metallicity. The dotted lines are the case with solar metallicity $Z = 0.019$. At given Z and increasing Z , H_{α} increases, Mg_2 and $hFei$ decrease (it is worth recalling here that higher values of imply lower values of $[Fe/H]$), whereas Mg_b is almost insensitive to Z and Z . In this respect Mg_b turns out to be the best age indicator of the group of four indices (see also the entries of Table 4). The same trends are found with the TP 96 SSPs. The major difference would be that the effect on H_{α} is exalted.

(vi) The enrichment law $Y = Z$. The Padova data-base of stellar tracks has been calculated assuming a suitable law of chemical enrichment $Y = Z$, i.e. the relation $Y - Y_p = (Z - Z_p)$, where Y_p and Z_p are the primordial helium and metal abundances, respectively, and ϵ is the enrichment ratio. If $Z_p = 0$ is an obvious choice, excluding the effect of primordial Pop III stars that in principle could alter both Y_p and Z_p (Maringo et al. 2002; Salvaterra & Ferrara 2003), the choice of Y_p and ϵ is more difficult. A recent observational estimate by Peimbert & Peimbert (2002) yields $Y_p = 0.23$ and $\epsilon = 2.1 - 0.5$. Bertelli et al. (1994) have adopted $Y_p = 0.23$ and $\epsilon = 2.5$ (Pagel 1989), whereas SGW C00 have chosen $Y_p = 0.23$ and $\epsilon = 2.25$ as in Girardi et al. (2000). Other data-bases of stellar tracks and SSPs have been calculated and/or assembled either explicitly or implicitly assuming similar enrichment laws, e.g. the SSPs by Worthey (1994) and TFW G00 in turn have $Y_p = 0.228$ and $\epsilon = 2.7$, whereas Maraston (1998) adopts $Y_p = 0.23$ and $\epsilon = 2.5$ but for extremely high metallicities for which adopts the Salasnich et al. (2000) prescription. In many other cases the $Y = Z$ relationship is simply ignored. Unfortunately no useful set of stellar tracks can be found in literature, in which a large range of metallicities are explored at constant Y . Basing on the few and limited set of stellar tracks to disposal, suffice it to note here that stellar models with the same Z and higher Y tends to be brighter and bluer than those of lower Y . This would immediately reflect onto the colours and indices of the associated SSPs. This is a point to keep in mind when exploring the effect of Z because depending on the chosen set of models, varying Z can actually mask also important effects of Y .

Final remark. The above discussion clarifies first that not all stellar models are equivalent (indeed important differences exist even among libraries calculated by the same group, see e.g. TP 96 and SGW C00 (the most relevant differences here are the opacities and the prescription for the mass-loss rate at the T-RGB)), second that details of stellar models might bear very much on the final correla-

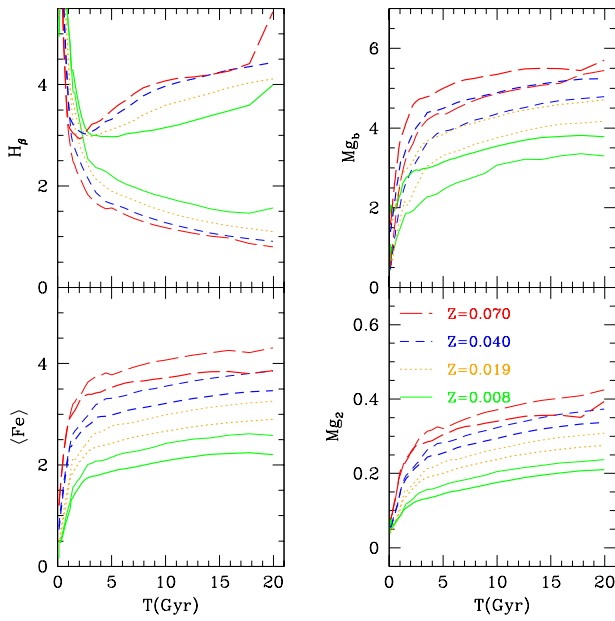


Fig. 10. Dependence of the indices H_{β} , Mg_2 , Mg_b , and $hFei$ on the age, metallicity and degree of enhancement. The metallicity levels are $Z = 0.008$ (solid lines), 0.019 (dotted-dashed lines), 0.04 (dashed lines), and 0.07 (long dashed lines). The thin lines are for $Z = 0$, whereas the thick lines are for $Z = 0.5$. The SSPs are those by SGW C00 with the corrections by TB 95.

tion between indices and metallicity and age. This latter point is not trivial considering that high metallicity stars (well above solar) could exist in the population mix of EGs, see Bressan et al. (1994). Finally, the effect of Z is of paramount importance and opposite to what expected from simple minded considerations.

8.3. The abundance patterns

Another important and obvious source of disagreement are the patterns of abundances especially when enhanced mixtures are adopted. As a matter of fact, a star index depends on the gravity, T_{eff} (that are function of the gross chemical parameters, Y and Z) and detailed chemical composition at the surface ([Fe/H] at least). This is particularly relevant when corrections are applied to pass from solar-scaled to enhanced mixtures. In other words, an index depends more on the detailed pattern of abundances adopted to derive the fitting functions than on the gross chemical parameters of the underlying stellar models.

Furthermore, comparing the distributions in age, metallicity and $[Fe/H]$ (Fig. 3) based on the SGW C00 indices with those by TFW G00 for their C^0O^+ model is not fully correct because the two patterns of abundances are not the same.

To clarify the subject we perform several experiments combining different sets of isochrones with different choices for the abundance patterns, the enhanced mixtures in particular.

8.3.1. Case A : The SGW C00 set of abundances

In this section we remind the reader that a new set of indices has been calculated adopting the isochrones by SGW C00 and the enhancement factor $\epsilon = 0.50$. Since the abundance pattern of these models has already been presented in Sect. 7.2 no more details are given here. In the following we will refer to the grids of the SGW C00 indices with $\epsilon = 0$, 0.3557 , and 0.50 as Case A (see the range of this grids in Sect. 7.2).

8.3.2. Case B : The C^0O^+ model of TFW G00

Since the TFW G00 indices are calculated from solar-scaled stellar models-SSPs on the top of which different degrees of enhancement are added by means of the TB 95 calibration (to a first approximation the effect of enhancement on stellar models is neglected) we have to recover the same situation. To this aim we adopt the SSPs by TP 96 up to the PAGB phases (see section 8.2 above), and the pattern of enhanced abundances as in the model by TFW G00 labelled C^0O^+ .

The abundance patterns presented by TFW G00 have three groups of elements:

Enhanced elements⁷ : N ; Mg ; Na ; Si ; Ti . They are indicated by TFW G00 as E elements;
Depressed elements⁸ (i.e. Fe-peak Group): Fe ; Ca ; Cr . They are denoted as D elements;
Fixed elements, which means solar-scaled.

Furthermore, different values can be assigned to C and O . In their model C^0O^+ , C belongs to the group of fixed elements whereas O to the group of enhanced elements.

To properly compare our results with those by TFW G00, we must establish the correspondence between our definition of ϵ with that adopted by TFW G00. According to their notation, our eq. (4) can be cast in the following way

$$[Fe/H] = [\epsilon = H] - A [\epsilon = Fe]$$

or

$$[Fe/H] = A [\epsilon = Fe]$$

at fixed $[\epsilon = H]$ where ϵ refers to the mass fraction of elements that are specifically enhanced and A is a generic constant of proportionality. This means that $A [\epsilon = Fe]$ corresponds to ϵ of eq. (4).

In TFW G00 the enhancement factor is let vary from $\epsilon = Fe$ = -0.30 to $\epsilon = Fe$ = 0.75 which means that the ratio $[O = H]$ increases from $\{0.021$ up to 0.053 , whereas $[C = H]$ remains equal to 0. It is worth noticing that the case with $\epsilon = Fe$ = -0.30 and $[O = H]$ = $\{0.021$ considered by TFW G00 actually corresponds to a decrease of the elements and $[O = H]$ with respect to the solar pattern.

⁷ They are scaled up by the same factor

⁸ They are scaled down by the same factor

In Table 5 (the analog of Table 4 in TFW G 00) we summarize the abundance ratios we have adopted to correct the indices according to their model C^0O^+ and our definition of Ξ given by eq. (13). Column n (1) gives the constant A . Column n (2) yields the enhancement factor ($\Xi = Fe$ or equivalently $\Xi = A$ in our notation). Columns (3) and (4) list the amount of depression and enhancement for E- and D-elements, respectively. Finally columns (5) through (8) give the mass fractions of C, O, Fe and enhanced-elements.

The range of age, metallicity and enhancement spanned by our new grid of indices based on the TP 96 SSPs is

0	T (Gyr)	20
0.008	Z	0.100 or 0.42
0.28		0.70 or 0.30 $[Fe/H] = 0.92$ ⁹

The grid contains four values of metallicity, namely $Z = 0.008$, $Z = 0.02$, $Z = 0.05$ and $Z = 0.1$ which correspond to $[Fe/H] = \{0.42, [Fe/H] = 0, [Fe/H] = 0.47, [Fe/H] = 0.92$ according to the TFW G 00 notation. For each metallicity we have corrected the indices by using eq. (13) for the different values of Ξ given in Table 5. Subsequently, we have interpolated among the four grids in steps of $\Xi = A$ $[Fe/H] = 0.02$ or equivalently $[Fe/H] = 0.03$. Finally, the age steps are the same of the original isochrones. These experiments allow us to test the effect of a simple enhancement scheme on the standard stellar models/SSPs. This type of models is referred to as Case B.

8.3.3. Case C : The TP 96 isochrones and the SGW C 00 mixture

Finally, we consider the case of indices calculated with the old SSPs of TP 96 and the mixtures of chemical abundances of SGW C 00, i.e. $\Xi = 0, 0.3557$, and 0.50 . The resulting grids are now given by:

0	T (Gyr)	20
0.008	Z	0.100 or 0.42 $[Fe/H] = 0.92$ ¹⁰
0.00		0.50

These sets of indices allow us to test the effect of a complex abundance scheme on standard SSPs. Models of this type are referred to as Case C.

⁹ We adopt $Z = 0.02$ and $X = 0.7000$ to replace Z with $[Fe/H]$, and the constant $A = 0.9288$ let us to shift between and $[Fe/H]$.

¹⁰ We adopt $Z = 0.02$ and $X = 0.7000$ to replace Z with $[Fe/H]$.

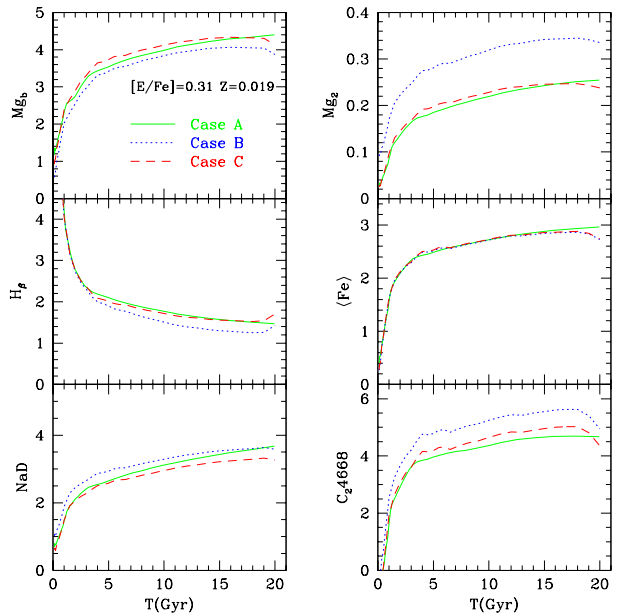


Fig. 11. Evolution of six indices (Mg_b , Mg_2 , H , $hFei$, NaD and C_24668) as function of the age according to the recipes of Cases A (solid lines), B (dotted lines), and C (long dashed lines) and limited to the solar metallicity $Z = 0.019$.

8.3.4. Comparing the indices of Cases A, B and C

In this section we present a quick comparison of the results we would obtain from the three cases above. In Fig. 11 we present the six indices under consideration as function of the age for the case with solar composition ($Z = 0.019$) and enhancement $[Fe/H] = 0.31$ (we adopt here the notation by TFW G 00). It is soon evident that Cases A and C which have the same pattern of abundances in the calculation of the indices yield nearly the same results despite the fact that they stand on different SSPs/isochrones. The largest difference is with Case B which has a different set of abundances. The difference is particularly remarkable for Mg_2 (top-right panel of Fig. 11). We would like to stress that this experiment clearly shows that the abundance ratios are the key parameter. The opposite conclusion reached by TFW G 00 is likely due to an insufficient exploration of the parameter space since they limit the analysis to varying only C and O. We show in Section 9.2 how the adoption of a particular set of abundance ratios would reflect on the age estimate.

8.4. Extrapolating grids of indices

There is another important point to be made that could bear very much on the final results, i.e. the way grids of stellar models/SSPs/indices are extrapolated from existing tabulations.

To illustrate the point let us have a close look to the extension made by TFW G 00 of the Worthey (1994) grid of SSPs already shown in the various panels of Fig. 9. The

Table 5. Element mass fractions in metals for non solar abundance ratios according to the model $C^{16}O^{+}$ of TFW G 00.

A	[E=Fe]	[D=H]	[E=H]	X _c =Z	X _o =Z	X _{Fe} =Z	X _E =Z
0.9288	{0.30	0.28	{0.021	0.174	0.433	0.137	0.252
0.9288	0.00	0.00	0.000	0.174	0.482	0.072	0.265
0.9288	0.32	{0.30	0.023	0.174	0.506	0.036	0.279
0.9288	0.75	{0.70	0.053	0.174	0.508	0.015	0.300

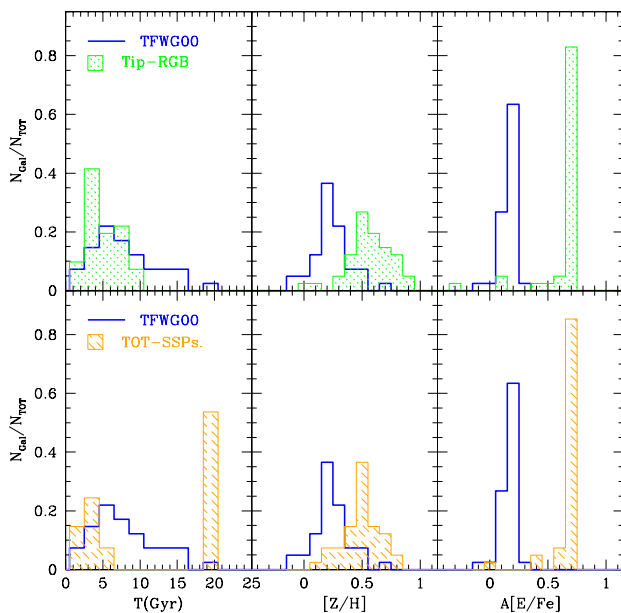


Fig. 12. The bottom three panels show the age T (in G yr), metallicity ($[Z=H]$) and enhancement ($A[E=Fe]$) distributions (from left to the right) for the Gonzalez (1993) sample of galaxies. The thick lines show the results of TFW G 00. The shaded histograms are the results for the Case B models, i.e. for the $C^{16}O^{+}$ -pattern of abundances and the complete SSPs of TP 96. The top three panels show the same but adopting the SSPs of TP 96 limited to the T-RGB. See the text for details.

The maximum age of the SSPs is 17 G yr and three values of metallicity are considered, i.e. $Z = 0.007, 0.02, 0.05$. For ages older than about 5 G yr the behavior of the various indices under examination is very smooth, almost linear in the two parameters. Basing on this, the linear extrapolation of the indices to older ages, higher metalicities, and higher values of seems to be reasonable. Indeed the grids have been extrapolated by TFW G 00 to ages up to 30 G yr and metalicities up to $Z = 0.07$.

However we have already discussed that stellar models, SSPs, and indices in turn are very sensitive to age and metallicity, and that past the T-RGB some unexpected evolutionary phases may appear largely affecting the regular trend of the indices in previous stages, at younger ages and/or lower metallicity. The effect is clear comparing the old SSPs/indices of TP 96 to those of SGW C 00 and the experiments on the indices that we have performed with the TP 96 SSPs truncated at different evolutionary phases.

Furthermore, we have already noticed that TFW G 00 grids of indices even in the age and metallicity ranges covered by the original Worthey (1994) models are much akin to the TP 96 ones truncated at the T-RGB.

Therefore the use of incomplete grids of stellar models and the straight extrapolation of stellar models/indices to much older ages and/or much higher metalicities might not be a safe procedure to adopt.

Only for the sake of argument, in the bottom panel of Fig. 12 we compare the distribution of age, metallicity and enhancement factor (the same notation of TFW G 00 is adopted for the sake of a quick comparison) for the Gonzalez sample of galaxies using the TFW G 00 grid (or the closest one to it, i.e. TP 96 stellar SSPs and TFW G 00 abundance pattern), and in the top panel of Fig. 12 we show the same but using SSPs of the TP 96 library truncated at the T-RGB. In the first case, the distributions in the three panels are much different from those of TFW G 00: in our models the age splits in two sub-groups, younger than about 5 G yr (35% of the total) and very old (65% of the total). It is soon evident that a partial agreement with TFW G 00 is possible only with the truncated TP 96 grid, whereas, when the full grid of models is adopted, Case B, the distribution differs from that of both Case A (already presented in Fig. 1) and TFW G 00.

8.5. Comparing ages, metalicities and s from various sources

The results obtained from the Minimum-Distance Method applied to the Gonzalez's sample and the different sets of theoretical indices are summarized in Fig. 13 and in Table C.1 described in the Appendix C and made available by the authors upon request. Unfortunately, each case yields different results due to the different assumption for the input SSPs and pattern of abundances. Looking at the cases in more detail, we note the following:

(i) Case A { Ages clusters in three groups, from 1 to 6 G yr, from 9 to 12 G yr, and 20 G yr, where about half of the population is found. The metallicity now goes from $[Z=H] = 0.0$ to $[Z=H] = 0.2$ and on the average it is lower than in TFW G 00. The enhancement factor peaks at $A[E=Fe] = 0.4$ about 0.2 dex higher than in TFW G 00.

(ii) Case B { Ages split in two well separated groups, younger than about 5 G yr and very old (at the grid limit); the metallicity peaks at about $[Z=H] = 0.5$, and $A[E=Fe] = 0.7$. In TFW G 00, the almost evenly distributed from 1 to 16 G yr with very few objects of 20 G yr, the

Metallicity is centered at $[Z/H] = 0.2$, i.e. a factor of two lower, the enhancement factor peaks at $A[\text{Fe}/\text{H}] = 0.2$, a factor of three lower.

(iii) Case C { Ages split in two groups, from 1 to 9 Gyr and 10 to 16 Gyr, with almost equal number of galaxies in each. No galaxy is found older than 16 Gyr. The distribution in metallicity is nearly the same as in TFWG00, only 0.1 dex lower, whereas the enhancement factor peaks at $A[\text{Fe}/\text{H}] = 0.4$ where the majority of galaxies are found with a minute tail extending down to $A[\text{Fe}/\text{H}] = 0$. This case is the only one, based on complete SSPs, getting sufficiently close to the results by TFWG00.

Comparing Case B to Case C the effect of different patterns of chemical abundances in the enhanced mix is revealed, whereas comparing Case A to Case C, the effect of different stellar models/ isochrones is highlighted. Both have a large impact on the assignment of ages, metallicities and degree of enhancement to the galaxies of the González (1993) sample.

The conclusion of this lengthy section is that the solution is highly model dependent. Model here means the pattern of basic ingredients, namely the stellar models, the companion isochrones and SSPs, the chemical composition and in particular the abundance ratios assumed in the mix, the Fitting Functions and the Response Functions in usage, together with some technical details such as the way the theoretical grids are assembled. Recovering the TFWG00 solution is possible only if their assumptions are strictly followed. In all other cases, the solutions are significantly different from that found by TFWG00. The tendency, however, is to predict a large fraction (up to 50% or more) of galaxies with old ages (say above 10 Gyr) instead of less than 30%. At this stage it is hard to decide which result has to be preferred.

9. What about using other indices? Is the solution unique?

Another important question to be addressed is whether different indices yield the same answer as far age, metallicity and enhancement factor are concerned. In so far we have analyzed the triplet H_β, HFeI and Mg_b because tighten to the González sample. However, several equally representative catalogs of galactic indices are available in literature, for instance the Trager "ID SP pristine" sample (Trager 1997), which allow us to derive the above parameters first for a larger number of galaxies and even more relevant here for different groups of indices.

In the analysis below we will consider six different indices (Mg_b, Mg₂, H_β, HFeI, NaD and C₂4668) and all possible combinations in groups of three. The inclusion of NaD and C₂4668 deserves some cautionary remarks. According to Thomas et al. (2003) both indices are not well calibrated. In addition to this, C₂4668 is very sensitive to the C abundance (TB 95) and NaD is contaminated by interstellar absorption (Maraston et al. 2003). The only advantage with these indices is their sensitivity to Z and (see the entries of Table 4). Keeping these caveats in mind, we

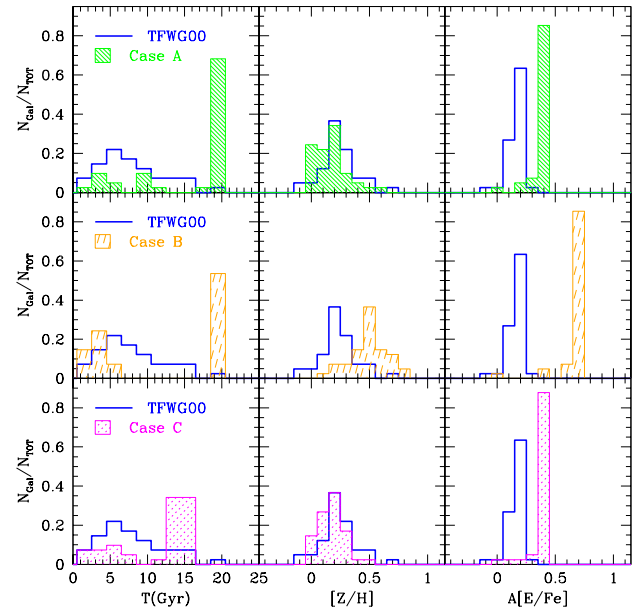


Fig. 13. Summary of the results for Cases A, B and C. The top three panels show the age (in Gyr), metallicity ($[Z/H]$) and enhancement ($A[\text{Fe}/\text{H}]$) distributions, from left to right for Case A models. The thick lines are the TFWG00 solution, drawn here for comparison. The middle three panels are the same but for Case B models. Finally the bottom three panels are the results for Case C models.

decided to make use of these indices, C₂4668 in particular, because, as shown in Fig. 15 below, the situation is not as bad as it may seem. The observational values are indeed well reproduced by their theoretical counterparts.

An index is considered to be eligible for this kind of analysis if its observational and theoretical value coincide within an uncertainty of 10%.

In Table 6 we summarize the results of the ranking analysis. Column (1) lists the indices, columns (2) through (4) yields the merit parameter of the observational vs. theoretical relationships: Y means a good correlation within 10% uncertainty, whereas N means a bad correlation. In addition to this, we have selected only those index-triplets having three good merit parameters. The ranking is made of all stellar models and abundance mixtures under consideration, namely Cases A, B and C. For each case there are several triplets meeting the constraint. They, however, change from case to case.

Specifically, in the case of the SGW C00 mixture and SSPs (Case A) the four combinations of indices H_β-Mg_b-Mg₂, H_β-Mg_b-C₂4668, Mg_b-Mg₂-C₂4668 and Mg_b-NaD-C₂4668 seem to be eligible to derive the age, metallicity and $A[\text{Fe}/\text{H}]$. In Case B, i.e. the TFWG00 mixture applied to the TP96 SSPs, good triplets are H_β-Mg_b-NaD, H_β-Mg_b-C₂4668, and H_β-Mg₂-C₂4668. Finally in Case C, the TP96 SSPs plus the SGW C00 abundances, the good triplets are: H_β-Mg_b-Mg₂, H_β-Mg_b-NaD, H_β-Mg_b-C₂4668, H_β-Mg₂-C₂4668 and Mg_b-Mg₂-C₂4668. Also in

Table 6. Ranking analysis of the index-triplets.

Index-Triplet	Case A	Case B	Case C
H hFeiM g _b	Y N Y	Y N Y	N N Y
H hFeiM g ₂	Y Y N	Y Y N	N Y N
H hFeiN aD	Y N Y	N N Y	N N Y
H hFeiC ₂ 4668	N N Y	Y N Y	N N Y
H M g _b M g ₂	Y Y Y	Y Y N	Y Y Y
H M g _b N aD	N Y Y	Y Y Y	Y Y Y
H M g _b C ₂ 4668	Y Y Y	Y Y Y	Y Y Y
H M g ₂ N aD	N N Y	Y N Y	Y N Y
H M g ₂ C ₂ 4668	Y N Y	Y Y Y	Y Y Y
H N aD C ₂ 4668	N N Y	N N Y	N N Y
hFeiM g _b M g ₂	N Y N	N Y N	N Y N
hFeiM g _b N aD	N Y Y	N Y Y	N Y Y
hFeiM g _b C ₂ 4668	N Y Y	N Y Y	N Y Y
hFeiM g ₂ N aD	N N Y	N N Y	N N Y
hFeiM g ₂ C ₂ 4668	N N Y	N N Y	N N Y
hFeiN aD C ₂ 4668	N Y Y	N N Y	N N Y
M g _b M g ₂ N aD	Y N Y	Y N Y	Y N Y
M g _b M g ₂ C ₂ 4668	Y Y Y	Y N Y	Y Y Y
M g _b N aD C ₂ 4668	Y Y Y	Y N Y	Y N Y
M g ₂ N aD C ₂ 4668	N Y Y	N Y N	N N Y

In this case we apply the Minimum-D instance M method. The analysis is made for all the galaxies of the Trager (1997) catalog using the various sources of SSPs and abundance patterns. No tabulations of the solution are presented here for the sake of brevity. In the Appendix C we shortly describe the content of Tables C 2, C 3 and C 4 that are made available by the authors upon request.

Limited to Case A, the results for the distribution of age, metallicity and enhancement factor are displayed in the various panels of Fig. 14. Each galaxy is identified by its list number in the Trager (1997) catalog (see also the first column of Table B 2 below). In each panel we show the range (the vertical bar) spanned by the determinations and their mean value (the full circle) obtained from the different triplets of indices. The top, mid and bottom pan-

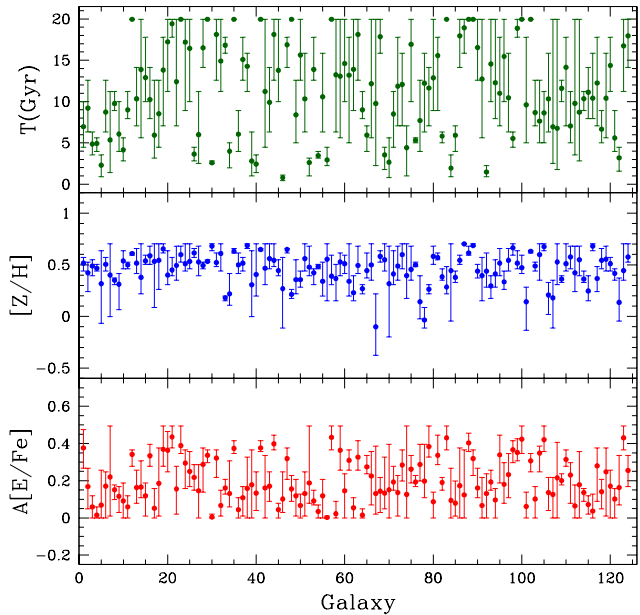


Fig. 14. Age, metallicity, and enhancement factor obtained from the Case A models but using different index-triplets, i.e. H -M g_b -M g₂, H -M g_b -N aD, M g_b -M g₂ -C₂4668 and M g_b -N aD -C₂4668. The full circles show the mean value of age, metallicity and enhancement factor estimated for each galaxy of the Trager 'IDSP pristine' sample whereas the vertical bars indicate the maximum and minimum values. Different triplets yield different results for most galaxies.

els shows the age, the metallicity, and the enhancement factor, respectively. Similar diagrams can be constructed also for Cases B and C with similar results. It is soon evident that a large spread exists among the determinations of the same parameter obtained from different triplets of indices.

Is the dispersion real? In the sense that each combination of indices is more sensitive to some specific property of the underlying stellar mix and therefore it traces the stellar component most contributing to the indices in question. Or despite the merit parameter not all triplets are actually good indicators? Finally, what about passing from Case A to Case B and to Case C? We seek to answer the above questions in the coming sections.

9.1. Is the dispersion real?

The experiments with SSPs truncated at different evolutionary stages, i.e. TO, T-RGB, post core HeB and total, may help understand whether the dispersion above is caused by a different response of triplets of indices to some specific evolutionary phase or group of stars. First we perform the analysis for Case A because it is based on the most updated grid of SSPs and self-consistent treatment of enhanced elements both in the stellar models and indices. With the five indices that have passed the merit test and on which the triplets of Case A have been

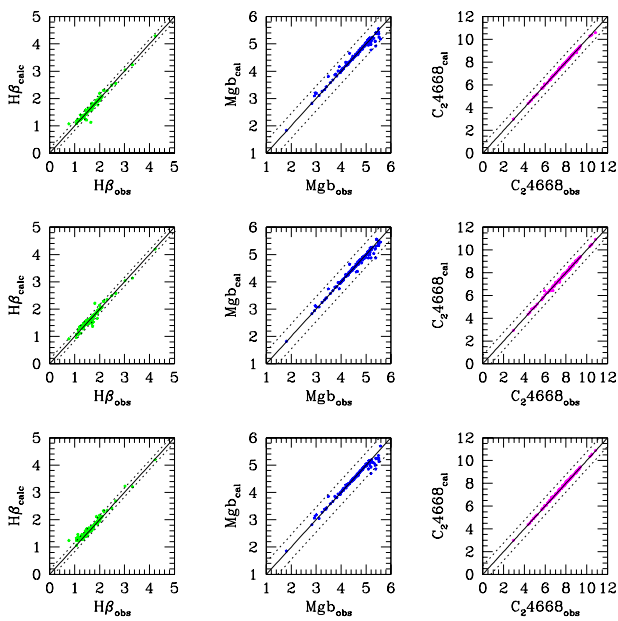


Fig. 15. Ranking test for the triplet $H - Mg_b - C_24668$ common to Cases A, B and C. The top panels are for Case A indices, i.e. the SGW C00 SSPs and pattern of abundances. The middle panels are for Case B, i.e. the TP 96 SSPs and TFW G00 C^0O^+ mixture. Finally, the bottom panels are for the TP 96 SSPs and the SGW C00 (Case C). In all cases the triplet $H - Mg_b - C_24668$ fulfills the ranking conditions.

constructed, namely H , Mg_b , Mg_2 , N_{AD} and C_24668 , the situation is as follows: (a) in all indices a substantial contributions comes from TO stars (about 2/3 for H and about 1/2 for Mg_b), and from the later phases (1/3 for H and nearly 1/2 for the remaining indices); (b) excluding ages younger than 3 Gyr at which all indices show strong variations, at older ages the dependence of all indices on the age becomes rather poor whereas that on the other two parameters is always significant. All this can be seen from the entries of Table 4 and the data in Figs. 1, 10, and 11. We have performed many numerical experiments using fictitious SSPs whose terminal stage is the TO, the RGB, and the P-AGB. They are not shown here for the sake of brevity. Despite the fact that some indices are sensitive to particular evolutionary phases, a large dispersion in age, metallicity and enhancement factor is always the result at varying the triplet of indices in use. Our conclusion is that small details of the grids, and the equal sensitivity of most indices to age, metallicity and enhancement degree, somehow weakens the practicalability of the M in m - D instance M method to assess the three parameters we are looking for. The dispersion in the solutions obtained from different triplets of indices is most likely of numerical nature. On the other hand since there are no strong arguments to prefer one triplet with respect to others (especially for the popular ones built with indices such as H , Mg_2 , Mg_b , $hFei$, etc.) the dispersion we find means that the solution is not really established.

Even keeping constant the stellar models/SSPs and transformations, ranking galaxies as function of age, metallicity and enhancement factor by means of the above technique is highly uncertain and questionable.

9.2. SSPs and abundance pattern

There is another point of severe embarrassment, i.e. at given total enhancement factor, the results much depend on the details of the abundance pattern of enhanced elements together with the source of SSPs. To illustrate this aspect of the problem, we perform the following experiment. First we isolate a index-triplet eligible according to our ranking screening and common to all the three Cases (A, B, and C). Looking at the entries of Table 6 we see that the sought triplet is H , Mg_b and C_24668 , for which we display in Fig. 15 the index-index correlation determining the merit parameter, and derive the age, the metallicity, and the enhancement factor according to Case A, Case B and Case C. Taking the age as a probe of the problem, we compare the ages derived from the same triplet of indices but different SSPs and abundance patterns. The results are shown in the three panels of Fig. 16. Passing from the combination Case A versus Case C (same abundance pattern but different SSPs shown in the top left panel) where the solution scatters around the line of equality most likely due to the differences in SSPs and details of the method in usage, to the combination Case C versus Case B (the same SSPs but different abundance pattern displayed in the top right panel) the ages derived with the SGW C00 mixture tend to be systematically older than those with the TFW G00 mixture, finally passing to the combination Case A versus Case B (different SSPs and patterns of abundances shown in the bottom left panel) nearly the same trend of the latter case is found which once again confirms that the underlying pattern of abundances is taking over all other details. Similar trends are found for the metallicity and the enhancement factor. This clarifies that at given total metallicity and enhancement factor, the results much depend on the assumptions made for the detailed pattern of abundances used to build the grids of theoretical indices. The problem seems to be somewhat circular and with no obvious way-out at least at this level of complexity.

9.3. The whole set of six indices

Since triplets of different combinations of the six indices H , Mg_b , Mg_2 , $hFei$, N_{AD} , and C_24668 yield different solutions for ages, metallicity and m , a last attempt is made using all the six indices at once applied to Case A models. The results are shown in the top panel of Fig. 17 and contained in Table C.5 shortly described in the Appendix C and made available upon request. Compared to the results for the same models obtained from the three indices H , Mg_b , and $hFei$ and presented in Fig. 13, the number of galaxies of very old age has decreased in favor of a sig-

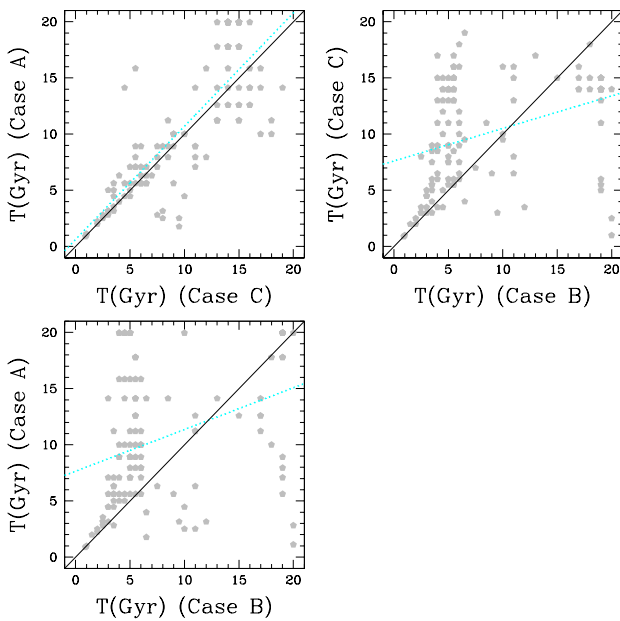


Fig. 16. Comparison between the ages (full dots) obtained from different sets of isochrones and different enhancement patterns, but adopting the same index-triplet shown in Fig. 15. The top-left panel compares Case A vs. Case C. The one to one relation and the linear best fit of the results are indicated by solid and dotted lines, respectively. The top-right panel shows the same but for Case C vs. Case B. Finally, the bottom-left panel displays Case A vs. Case B.

in a faint component of younger ages; the metallicity is on the average 0.3 dex higher, and goes from zero to about 0.5. Even for Case A models, the situation is not as bad as it was before.

10. Breaking the age-metallicity degeneracy by hand

What we learn from the systematic analysis of the problem is that the simultaneous use of three indices (in many combinations of these) to infer the age, metallicity and degree of enhancement with the Minimum-Distance M method leads to very unstable results that much depend on details of the adopted SSPs and the intrinsic degeneracy of the problem. The major difficulty is the low and nearly equal sensitivity of many indices to the age, metallicity and (see the entries of Table 4). This weakens the applicability of the straight Minimum-Distance M method and tends to yield numerical solutions at the limits of the theoretical grids. The difficulty is partially removed by using more indices instead of triplets.

This suggests us a slightly different procedure (namely the Recursive Minimum-Distance M method). Taking advantage of the high sensitivity of C_24668 and $N\alpha D$ to Z and the relative lower sensitivity of Mg_2 , Mg_b and $hFei$ to Z (see the entries of Table 4), of the experiments made with different triplets, and also of the improvement reached us-

ing the whole set of indices instead of triplets, we made use of the mean values of age, metallicity and Z derived from different combinations of indices and break the problem in three steps:

(i) given a galaxy with observational values for the indices $H\alpha$, C_24668 , $N\alpha D$, Mg_2 , Mg_b and $hFei$, first we derive from different pairs of indices (C_24668 and $N\alpha D$ combined with Mg_2 , Mg_b and $hFei$ respectively) the mean value for Z_1 and T_1 using the Minimum-Distance M method reduced to only these two quantities and neglecting for the time being the age dependence.

(ii) The mean values of Z_1 and T_1 derived in this way are then used to construct the function $H(Z_1; T_1; T)$ and to solve the equation $H_0 = H(Z_1; T_1; T)$ for the age T_1 .

(iii) This value of the age is then plugged into step (i) and a new pair of mean Z_2 and T_2 is derived and inserted into step (ii) to get a new value of T_2 . The procedure is iterated till the solution becomes stable.

The intrinsic age-metallicity degeneracy has been broken by hand and the solution is better constrained. To illustrate the advantages offered by the Recursive Minimum-Distance M method we apply it to Case A models and the Trager (1997) galaxies. The results are displayed in the panels [1], [2] and [3] of Fig. 17. Panel [1] shows the mean values for the age, metallicity and Z derived from the different pairs of indices as described in steps (i) and (ii) above. Completing the three steps we get the solution shown in panel [2]. Finally, iterating once more the whole procedure we obtain the solution displayed in panel [3]. In two iterations the solution has become stable. Comparing the results of Fig. 17 with the starting mean values, we may notice how the results change thanks to the new resolving method.

Passing now to Case B and Case C the final distributions are not the same both with respect to Case A and with respect of each other, but this is entirely due to the different SSPs and abundance patterns for the elements. All the results obtained with the Recursive Minimum-Distance M method are summarized in Table B 2 given in the Appendix B.

The uncertainty and circularity caused by different patterns of elements at given total enhancement factor cannot of course be ruled out. The net advantage of the iterative procedure is that the uncertainty introduced by the little resolving power of many indices as far as age, metallicity, and degree of enhancement are concerned is significantly reduced.

If indices like C_24668 and $N\alpha D$ are not available (or have to be discarded), a preliminary analysis should single out the index in the set to dispose having the highest sensitivity to one of parameters under consideration in order to reduce the number of freedom-degrees of the problem and then apply a suitable iterative technique. This way of proceeding ought to be preferred to the straight application of the Minimum-Distance M method or similar procedures.

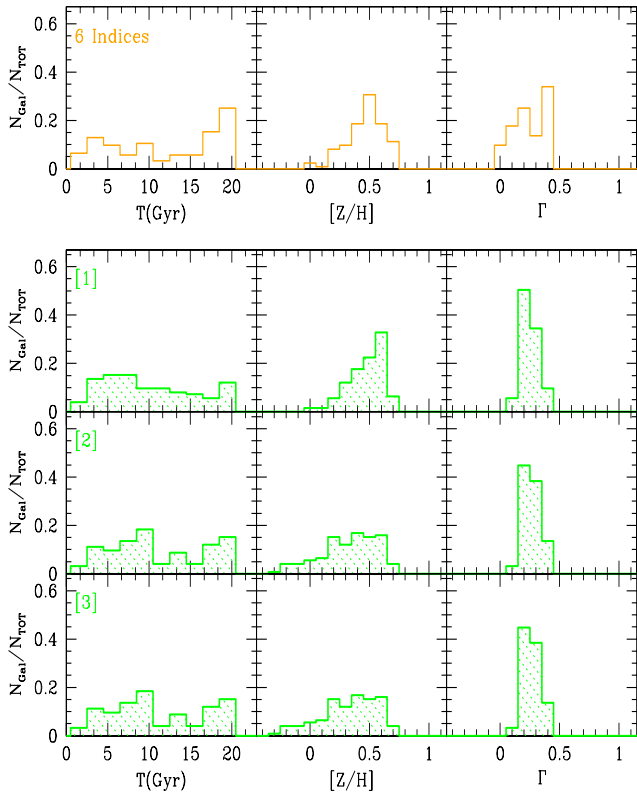


Fig. 17. Top panel: solutions obtained by using six indices at the same time instead of triplets as in the previous analyses. Three bottom panels [1], [2] and [3]: The Recursive Minimum-D Instance Method at work. Panel [1] shows the initial solution: provisional mean values of Z_1 and Γ_1 are derived from the pair C_24668 and N_{AD} combined respectively with M_{g2} , M_{g3} and hFei , neglecting the age dependence and solving the equation $H_1(Z_1; \Gamma_1; T)$ for the age T_1 . Panel [2] shows the first iteration in which new mean values of Z_2 and Γ_2 obtained from the above pairs of indices in which the age T_1 is inserted and solving the equation $H_2(Z_2; \Gamma_2; T)$ for the age T_2 . Panel [3] is the same but for the second iteration. The solution has become stable. See the text for more details. The shaded histograms show the results of this procedure applied to Case A models.

11. A few remarks on the two indices diagnostic

The two-indices planes are customarily used to interpret the observational data of galaxies and star clusters. Popular planes are the H or H_F vs. hFei or $[MgFe]$ or M_{g3} to derive the age and mean metallicity (Bressan et al. 1996; González 1993; Trager et al. 2000b), and the hFei vs. M_{g2} to assess the degree of enhancement (Worley 1992; González 1993; Weiss et al. 1995).

The two-indices diagnostics suffers the same uncertainty encountered with the Minimum-D Instance Method, however at a lower level of complexity because one of the parameters is hidden. At the light of the above discussion, the best diagnostic plane to use is the H vs. C_24668 plane and a series of these at varying Γ . With aid of H vs.

C_24668 () we can bracket the possible ranges spanned by the three parameters in question. Only for the sake of illustration, we display in Fig. 18 the plane H vs. C_24668 for $\Gamma = 0$ (top panel) and $\Gamma = 0.35$ (bottom panel) on which the galaxies of the Trager 'IDSP pristine' are plotted. As already amply discussed in the previous sections, while the resolving power of C_24668 concerning the metallicity is always very good (with some dependence on Γ), the resolving power of H concerning the age is very poor as the age gets older than about 5 Gyr. The eye inspection of this plane would indicate that the majority of galaxies seem to be older than about 5 Gyr and younger than about 15 Gyr for $\Gamma = 0$, and to fall in the range 15 to 20 Gyr for $\Gamma = 0.35$. Their metallicity seems to be confined between $Z = 0.04$ and 0.07. However, the arguments presented in the previous sections lead us to say that these are only crude estimates of the real values. Other diagnostic planes can be constructed, e.g. the widely used H vs. hFei or H_F vs. hFei (it is worth reminding the reader that H_F is considered to be a better age indicator than H , to be proved anyhow, and that the resolving power of hFei for the metallicity is much lower than that of C_24668), and other samples of galaxies can be analyzed, e.g. the Kuntschner (2001) sample of galaxies for the Fornax cluster, with no significant improvement of the overall situation.

12. Summary and concluding remarks

In this study we have investigated the ability of absorption line indices to assess the metallicity Z , the iron content $[\text{Fe}/\text{H}]$ and, in turn, and the age of elliptical galaxies. The analysis has been developed through several steps:

(i) First of all we have generated grids of indices based on SSPs calculated with chemical composition and opacities enhanced in elements, and transformations in which the same chemical mixtures have been adopted. The SSPs and associated indices are for three degrees of enhancement, i.e. $\Gamma = 0$, $\Gamma = 0.3557$, and $\Gamma = 0.50$.

(ii) Secondly, we have assessed the response of the indices to variations of age, metallicity, and Γ and found that most of the indices have similar response to three parameters but for a few of them which are definitely more sensitive to metallicity and enhancement. It is worth calling attention that most indices are evenly and weakly depending on the age over large ranges. This is the most crucial aspect of the problem.

(iii) Applying the new grids of SSPs/indices to the popular sample of EGS by González (1993) we have found distributions of age, metallicity and enhancement factors that were too different with respect to previous studies (e.g. TFWG00) of the same data to be simply explained in terms of the different stellar models, SSPs, abundance patterns. This spurred a systematic analysis of the whole problem, in which we have examined the effect of the stellar models and SSPs in use, the contribution to the integrated indices of SSPs by stars in different evolutionary phases (TO, T-RGB, HeB, TP-AGB, and later), the de-

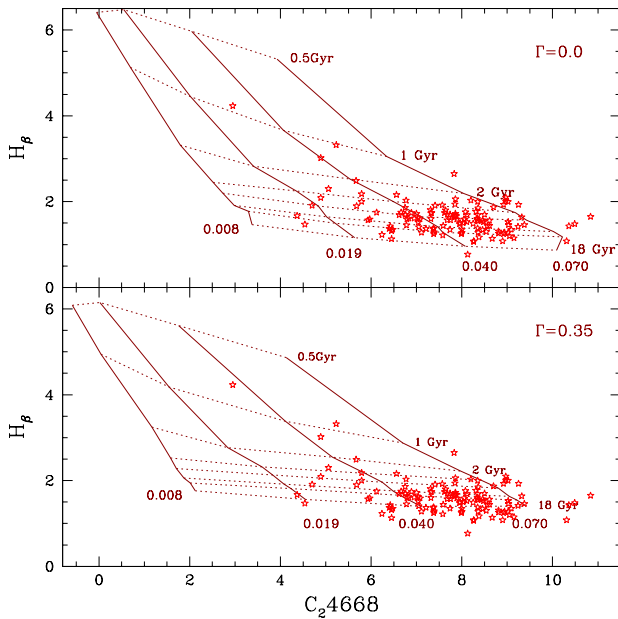


Fig. 18. The H_{β} vs. C_24668 planes for $R = 0$ (top panel) and $R = 0.35$ (bottom panel). The solid lines are the loci of equal metallicity, whereas the dotted lines are the loci of equal age as indicated. The theoretical indices on display are those of Case A. The empty stars are the data of the galaxies of the Trager 'ID SP pristine' sample. As already amply discussed in the text, while the resolving power of C_24668 concerning the metallicity is always very good (with some dependence on R), the resolving power of H_{β} concerning the age gets very poor as the age gets older than about 5 Gyr.

gree of enhancement in α -elements and the detailed pattern of abundances at given total enhancement factor, the technique adopted to extend (extrapolate) existing grids of SSP indices to ages, metallicity, enhancement factors not covered by the original models. The results of all this, is that each of the ingredients above bears very much on the final assignment of age metallicity and enhancement factor to individual galaxies, showing that the final result is very sensitive to many details. Amazingly enough, the problem becomes more and more uncertain at increasing complexity of the underlying stellar models and SSP grids, and sophistication in the abundance patterns.

(iv) The degree of enhancement poses another crucial question because the results much depend on the specific way in which the abundance pattern is built up at given total degree of enhancement. The argument is somewhat circular and cannot be easily solved, unless we have additional information on the relative abundances of the enhanced elements.

(v) What we learn from this systematical analysis is that the solution is highly model dependent, cf. the results obtained for the same sample of galaxies (Gonzalez 1993) passing from TFWG00, to Thomas et al. (2003), and the many cases we have discussed in the text at varying source of SSPs and pattern of abundances. In general

as far as ages are concerned, there is always a good fraction of galaxies with genuine old ages (the absolute value is less of a problem here), in contrast to the results by TFWG00 in which only less than about 30% of the whole sample were older than say 10 Gyr. The result is somehow unique to TFWG00 because it entirely rests on the SSPs by Worthey (1994). Other more sophisticated SSPs lead to different age (and metallicity and enhancement factor) distributions.

(vi) In addition to this, we have addressed the question whether the solution found for age metallicity, and enhancement factor is independent of the triplet of indices one has been using. The answer is of course no, in the sense that different triplets having a different resolving power leads to different results. Part of the difficulty resides in the Minimum-Distance Method itself which turns out to be inadequate to handle situations in which small variations in the observational and/or theoretical indices imply large variations in the age, metallicity and degree of enhancement. To cope with this difficulty we tried to estimate ages, metallicity, and enhancement in elements by simultaneously fitting many indices (six in our case). Though the situation gets better, it is not fully satisfactory.

(vii) On the basis of the above analysis and taking advantage from the distinct sensitivity of a few indices (C_24668 and N_{H} in our sample) to metallicity and enhancement factor, we propose a slightly different procedure which recursively applies the Minimum-Distance Method to the indices most sensitive to Z and α , and solves directly for the age. The merit of this procedure that it may help stabilize the solutions. We are inclined to consider this solutions as the one getting closer to reality.

(viii) Needless to say that the results still depend on the input SSPs and calibration in use, but this is a point of uncertainty that cannot be easily proved unless one has independent assessments of the quality of stellar models and calibrations.

(ix) There is another important remark to made about the use of SSPs to simulate the complexity of a real galaxy. We have already touched upon this topic in Sect. 7.2, but it should be stressed once more here. In real galaxies, even in the case of EGs, a mix of stellar populations with different ages and chemical properties is likely to co-exist. Therefore the approximation to SSP is no longer valid and SSPs should be replaced by galactic models incorporating the history of star formation and chemical enrichment and the indices to be used should take into account the contribution from all stellar components. Some of the properties shown in SSPs, especially those caused by non standard evolutionary stages (e.g. reversal of indices like H_{β} at increasing age and metallicity), that now have the same weight in the total balance of the resolving technique, are likely to smear out in the complex mix of stars because the contribution by each SSPs is proportional to the number of stars in the different age and metallicity bins. Integrated indices from real galaxies have been calculated by Tantalo

et al. (1998b) but never applied to this kind of analysis. This is a point that should be carefully investigated.

(x) There is one remark to be made. According to the results of this analysis and of previous ones as well, the conclusion one would draw is that EGs span very large ranges of age (and also of metallicity and enhancement in elements). The age is, however, the most embarrassing result. Does it means that in galaxies, for which formal ages younger than the typical age of globular clusters (say 13–15 Gyr) are found, the bulk of stars have been formed at such young ages or there are effects to be taken into account? The question has been addressed for the first time by Bressan et al. (1996), explored in more detail by Longhetti et al. (2000), and also discussed by TFWG00. The question is: how much a recent, minute episode of star formation, engaging a small fraction of the total mass, may alter the indices of an otherwise old population of stars in EGs? The analyses was made by superposing to the indices of an old population of stars the variation caused by a recent episode of star formation. The results is that indices like H are strongly affected by even small percentages of young stars: as long as star formation is active they jump to very high values and when star formation is over the fall back to the original value on a time scale of about 1 Gyr. Other indices like Mg_2 , $hFei$ are much less affected even if the companion chemical enrichment may somewhat change them. In diagnostics planes like H vs. $hFei$ the galaxy performs an extended loop elongated towards the H axis, thus causing an artificial dispersion which could be interpreted as an age dispersion, whereas what we really seeing is the transient phase associated to the temporary stellar activity. The implication of this have never been fully assessed with complete simulations of later star forming episodes of different intensity and age superposed to an old one. Work on this topic is underway (Tantalo & Chiosi 2003, in preparation).

Acknowledgements. This study has been funded by the Italian Ministry of Education, University, and Research (MIUR), and the University of Padua under the special contract "Formation and evolution of elliptical galaxies: the age problem".

References

Anders, E. & Grevesse, N. 1989, *Geochim. Cosmochim. Acta*, 53, 197

Barbuy, B. 1994, *ApJ*, 430, 218

Bender, R., Ziegler, B., & Bruzual, G. 1996, *ApJL*, 463, L51

Bertelli, G., Bressan, A., Chiosi, C., Fagotto, F., & Nasi, E. 1994, *A&AS*, 106, 275

Borges, C. A., Idiart, T. P., de Freitas Padreco, J. A., & Thevein, F. 1995, *AJ*, 110, 2408

Bressan, A., Chiosi, C., & Fagotto, F. 1994, *ApJS*, 94, 63

Bressan, A., Chiosi, C., & Tantalo, R. 1996, *A&A*, 311, 425

Brocato, E., Matteucci, F., Mazzitelli, I., & Tomabene, A. 1990, *ApJ*, 349, 458

Burstein, D., Bertola, F., Buson, L. M., Faber, S. M., & Lauer, T. R. 1988, *ApJ*, 328, 440

Burstein, D., Faber, S. M., Gaskell, C. M., & Krumm, N. 1984, *ApJ*, 287, 586

Buzzoni, A. 1989, *ApJS*, 71, 817

Castellani, V. & Tomabene, A. 1991, *ApJ*, 381, 393

Charlot, S. & Bruzual, G. 1991, *ApJ*, 367, 126

Chiosi, C., Bertelli, G., & Bressan, A. 1992, *ARA&A*, 30, 235

Chiosi, C. & Carraro, G. 2002, *MNRAS*, 335, 335

Davies, R. L., Kuntschner, H., Elmstell, E., et al. 2001, *ApJL*, 548, L33

Dorman, B., Rood, R. T., & O'Connell, R. W. 1993, *A&A*, 419, 516

Faber, S. M., Friel, E. D., Burstein, D., & Gaskell, C. M. 1985, *ApJS*, 57, 711

Faber, S. M., Worthey, G., & Gonzalez, J. J. 1992, in *The Stellar Population of Galaxies*, ed. B. Barbuy & A. Renzini, IAU Symp. 149 (Kluwer Academic Publishers: Dordrecht), 255

Fagotto, F., Bressan, A., Bertelli, G., & Chiosi, C. 1994, *A&AS*, 105, 39

Girardi, L. & Bertelli, G. 1998, *MNRAS*, 300, 533

Girardi, L., Bressan, A., Bertelli, G., & Chiosi, C. 2000, *A&AS*, 141, 371

Girardi, L., Bressan, A., Chiosi, C., Bertelli, G., & Nasi, E. 1996, *A&A*, 117, 113

Gonzalez, J. J. 1993, PhD thesis, University of California, Santa Cruz

Green, E., Demarque, P., & King, C. 1987, *The revised Yale isochrones and luminosity functions* (New Haven: Yale Observatory, 1987)

Greggio, L. & Renzini, A. 1983, *A&A*, 118, 217

— 1990, *ApJ*, 364, 599

Grevesse, N. 1991, *A&A*, 242, 488

Grevesse, N. & Noels, A. 1993, *Phys. Scr.*, 47, 133

Horch, E., Demarque, P., & Pinsonneault, M. 1992, *ApJ*, 388, L53

Idiart, T. P. & de Freitas Padreco, J. A. 1995, *AJ*, 109, 2218

Jorgensen, I. 1999, *MNRAS*, 306, 607

Kuntschner, H. 1998, PhD thesis, Univ. of Durham

— 2000, *MNRAS*, 315, 184

— 2001, *Astrophys. Space. Sci.*, 276, 885

Kuntschner, H. & Davies, R. L. 1998, *MNRAS*, 295, L29

Kuntschner, H., Lucey, J. R., Smith, R. J., Hudson, M. J., & Davies, R. L. 2001, *MNRAS*, 323, 615

Larson, R. B. 1974, *MNRAS*, 142, 501

Leitherer, C., Alloin, D., van Eyselen, U. F., et al. 1996, *PAASP*, 108, 996

Longhetti, M., Bressan, A., Chiosi, C., & Ramazzotti, R. 2000, *A&A*, 353, 917

Maraston, C. 1998, *MNRAS*, 300, 872

Maraston, C., Greggio, L., Renzini, A., et al. 2003, *MNRAS*, astro-ph/0209220

Marigo, P., Chiosi, C., & Kudritzki, R.-P. 2002, *A&A*, 617

Matteucci, F. 1994, *A&A*, 154, 279

— 1997, *Fundam. Cosm. Phys.*, 17, 283

Matteucci, F., Ponzone, R., & Gibson, B. K. 1998, *A & A*, 335, 855

Pagel, B. 1989, in *Evolutionary Phenomena in Galaxies*, ed. J. Beckman & B. Pagel (Cambridge: Cambridge University Press), 201

Peimbert, A. & Peimbert, M. 2002, 250

Poggianti, B., Bridges, T., Mobasher, B., et al. 2001, *ApJ*, 562, 689, (astro-ph/0107158)

Reimers, D. 1975, *Mém. Soc. R. Sci. Liège*, ser. 6, 8, 369

Renzini, A. & Buzzoni, A. 1986, in *Spectral Evolution of Galaxies*, ed. C. Chiosi & A. Renzini (Dordrecht: Reidel), 213

Salasnich, B., Girardi, L., Weiss, A., & Chiosi, C. 2000, *A & A*, 361, 1023, (SGW C 00)

Salvaterra, R. & Ferrara, A. 2003, *MNRAS*, in press, astro-ph/0302285

Tantalo, R. 1998, PhD thesis, Univ. of Padova

Tantalo, R. & Chiosi, C. 2003, submitted

Tantalo, R., Chiosi, C., & Bressan, A. 1998a, *A & A*, 333, 419

Tantalo, R., Chiosi, C., Bressan, A., Marigo, P., & Portinari, L. 1998b, *A & A*, 335, 823

Thomasson, D. & Maraston, C. 2003, *A & A*, astro-ph/0302063

Thomasson, D., Maraston, C., & Bender, R. 2003, *MNRAS*, astro-ph/0209250 (TM B 03)

Trager, S. 1997, PhD thesis, Univ. of California, Santa Cruz

Trager, S. C., Faber, S. M., Worthey, G., & Gonzalez, J. J. 2000a, *AJ*, 120, 165

| . 2000b, *AJ*, 119, 1645, (TFW G 00)

Trippico, M. J. & Bell, R. A. 1995, *AJ*, 110, 3035, (TB 95)

Vandenbergh, D. 1985, *ApJS*, 58, 711

Vandenbergh, D. & Bell, R. 1985, *ApJS*, 58, 561

Vandenbergh, D. & Laskarides, P. 1987, *ApJS*, 64, 103

Vassiliadis, D. A. & Wood, P. R. 1993, *ApJ*, 413, 641

Vazdekis, A., Kuntschner, H., Davies, R. L., et al. 2001, *ApJ*, 551, 127

Weiss, A., Peletier, R. F., & Matteucci, F. 1995, *A & A*, 296, 73

Worthey, G. 1992, PhD thesis, Univ. of California

| . 1994, *ApJS*, 95, 107

Worthey, G., Faber, S. M., & Gonzalez, J. J. 1992, *ApJ*, 398, 69

Worthey, G., Faber, S. M., Gonzalez, J. J., & Burstein, D. 1994, *ApJS*, 94, 687

Worthey, G. & Ottaviani, D. 1997, *ApJS*, 111, 377

Ziegler, B. L. & Bender, R. 1997, *MNRAS*, 291, 527

Appendix A :

Table A.1: Large tabulations of the complete set of indices on the Lick system for the SGW C 00 SSPs and the TB 95 corrections. Column (1): ; column (2): Metallicity Z ; column (3) Age (in Gyr); column (4) CN₁; column (5): CN₂; column (6): Ca4227; column (7): G 4300; column (8): Fe4383; column (9): Ca4455; column (10): Fe4531; column (11): C₂4668; column

(12): H ; column (13): Fe5015; column (14): Mg₁; column (15): Mg₂; column (16): Mg_b; column (17): Fe5270; column (18): Fe5335; column (19): Fe5406; column (20): Fe5709; column (21): Fe5782; column (22): NaD; column (23): TiO₁; column (24): TiO₂; column (25): H_A; column (26): H_A; column (27): H_F; column (28): H_F; column (29): hFei; column (30): MgFe]; column (31): MgFe]. The definition of hFei, MgFe] and MgFe] are

$$hFei = 0.5 (Fe5207 + Fe5335)$$

$$MgFe] = \frac{p}{Mg_b} (0.5 Fe5207 + 0.5 Fe5335)$$

and

$$MgFe] = \frac{p}{Mg_b} (0.72 Fe5207 + 0.28 Fe5335)$$

The following metallicities Z and enhancement factors are considered: $Z = 0.008, 0.019, 0.040$ and 0.070 ; $= 0, 0.35$ and 0.5 . Table available upon request or on the web site <http://dipastro.pd.astro.it/galadriel>.

Appendix B :

The appendix contains the data and solutions for age, metallicity and degree of enhancement for the Gonzalez (1993) list of galaxies we have discussed in Section 7.3, those of the TFW G 00 sample studied in Section 8, and those of the same list presented in Section 9.

Table B 1: Data and solutions for the Gonzalez (1993) $R_e = 8$ sample. Column (1) and (2) show the progressive number associated to each galaxies as indicated. Columns (3) through (5) and (6) through (8) give the values of the observational and theoretical indices respectively. Columns (9) through (11) give the results from the Minimum-Distance Method, namely: T (T), $Z = H]$ ($Z = H]$) and $()$.

Table B 2: Final solution obtained with the Mean Recursive Minimum-Distance Method as described in Sec. 10. Columns (1)–(6) and columns (2)–(7) show the progressive number and the name of the galaxies. Columns (3)–(8), (4)–(9), (5)–(10) give the ages, the ratio $Z = H]$ and the value of $A E = F e] = .$

Appendix C :

Table C 1: Theoretical indices and solutions obtained from Cases A, B and C for the Gonzalez sample. The first two columns in each group are the same as in Table B 1. Columns (3) through (5) give the theoretical indices: H, hFei and Mg_b, respectively, whereas columns (6) through (8) list the age T in Gyr, $Z = H]$ and $A E = F e]$ (i.e.) (where $A = 0.9288$ for Case A models). Table available upon request.

Tables C.2, C.3 and C.4: Solutions obtained from the Minimum-Distance method applied to the Trager\IDS "Pristine" sample, for Case A, Case B and Case C, respectively. Columns (1) gives the progressive number associated to each galaxy in the sample (column 2). For each index-triplets as appropriate for Case A, Case B and Case C listed in Table 6, the first, second and third columns give the ages in G yr, the ratio $[Z=H]$ and the value of $A(E=F)e]$ = . Table available upon request.

Table C.5: Solutions obtained from the Minimum-Distance method applied to the Trager\IDS "Pristine" sample using Case A models and imposing the simultaneous fit of six indices. Column (1) lists the progressive number associated to each galaxy in the sample, column (2) gives the name, columns (3), (4) and (5) give the age in G yr, the ratio $[Z=H]$ and the value of $A(E=F)e]$ = , respectively. Table available upon request.

Table B.1. Solutions for the Gonzalez (1993) sample obtained using the SGWC00 SSPs

Num.	Name	H _{obs}	H	hFei _{obs}	hFei	M _{g_{obs}}	M _{g_b}	H _{th}	hFei _{th}	M _{g_{th}}	T	T	[Z=H] ₊	[Z=H] ₋		
1	221	2.31	0.05	2.745	0.06	2.96	0.04	2.34861	2.76088	2.98401	2.512	0.1530	0.2628	0.044	0.0000	0.0049
2	224	1.67	0.07	3.095	0.08	4.85	0.04	1.65684	3.19291	4.71148	19.953	0.0000	0.1748	0.022	0.3663	0.0050
3	315	1.74	0.06	2.885	0.09	4.84	0.05	1.67970	3.09031	4.61690	19.953	0.0000	0.1088	0.022	0.3663	0.0050
4	507	1.73	0.09	2.775	0.19	4.52	0.09	1.74545	2.88046	4.40589	19.953	0.0000	-0.0232	0.033	0.3663	0.0050
5	547	1.58	0.07	2.815	0.11	5.02	0.05	1.66446	3.15871	4.67995	19.953	0.0000	0.1528	0.022	0.3663	0.0049
6	584	2.08	0.05	2.900	0.06	4.33	0.04	2.05686	2.93217	4.32003	8.913	3.0910	0.1968	0.110	0.3762	0.0049
7	636	1.89	0.04	3.030	0.07	4.20	0.04	1.88657	3.02486	4.20124	5.623	0.6490	0.3288	0.044	0.3069	0.0198
8	720	1.77	0.12	2.870	0.18	5.17	0.11	1.83881	3.25952	4.79332	19.953	0.0000	0.2188	0.055	0.3762	0.0050
9	821	1.66	0.04	2.945	0.07	4.53	0.05	1.70255	2.98770	4.52232	19.953	0.0000	0.0428	0.011	0.3663	0.0000
10	1453	1.60	0.06	2.975	0.09	4.95	0.05	1.65684	3.19291	4.71148	19.953	0.0000	0.1748	0.022	0.3663	0.0000
11	1600	1.55	0.07	3.055	0.11	5.13	0.07	1.62637	3.32972	4.83759	19.953	1.0850	0.2628	0.022	0.3663	0.0049
12	1700	2.11	0.05	3.000	0.07	4.15	0.04	2.12882	3.01823	4.14089	3.162	0.4095	0.4608	0.066	0.3564	0.0099
13	2300	1.68	0.06	2.965	0.09	4.98	0.05	1.65684	3.19291	4.71148	19.953	0.0000	0.1748	0.022	0.3663	0.0050
14	2778	1.77	0.08	2.850	0.11	4.70	0.05	1.70255	2.98770	4.52232	19.953	0.0000	0.0428	0.022	0.3663	0.0050
15	3377	2.09	0.05	2.605	0.06	3.99	0.04	2.07272	2.61558	3.97209	10.000	5.5200	-0.0452	0.099	0.3762	0.0049
16	3379	1.62	0.05	2.855	0.06	4.78	0.03	1.68732	3.05610	4.58537	19.953	0.0000	0.0868	0.022	0.3663	0.0049
17	3608	1.69	0.06	2.940	0.08	4.61	0.05	1.69494	3.02190	4.55384	19.953	0.0000	0.0648	0.011	0.3663	0.0000
18	3818	1.71	0.08	2.970	0.11	4.88	0.06	1.66446	3.15871	4.67995	19.953	0.0000	0.1528	0.022	0.3663	0.0050
19	4261	1.34	0.06	3.010	0.08	5.11	0.05	1.42515	3.33153	4.81878	19.953	0.0000	0.2628	0.011	0.3564	0.0000
20	4278	1.56	0.05	2.685	0.07	4.92	0.04	1.51176	3.02364	4.53515	19.953	0.0000	0.0648	0.022	0.3564	0.0049
21	4374	1.51	0.04	2.815	0.06	4.78	0.03	1.51176	3.02364	4.53515	19.953	0.0000	0.0648	0.011	0.3564	0.0000
22	4472	1.62	0.06	2.905	0.11	4.85	0.07	1.67208	3.12451	4.64843	19.953	0.0000	0.1308	0.022	0.3663	0.0000
23	4478	1.84	0.06	2.935	0.07	4.33	0.05	1.85086	2.92670	4.35318	11.220	2.0705	0.1308	0.088	0.3663	0.0049
24	4489	2.39	0.07	2.665	0.10	3.21	0.06	2.38245	2.65524	3.21139	2.512	0.2895	0.2408	0.077	0.1584	0.0347
25	4552	1.47	0.05	2.985	0.06	5.15	0.04	1.43477	3.29732	4.78727	19.953	1.0850	0.2408	0.022	0.3564	0.0049
26	4649	1.40	0.05	3.010	0.06	5.33	0.04	1.42097	3.44115	4.92814	17.783	0.0000	0.3508	0.011	0.3564	0.0000
27	4697	1.75	0.07	2.770	0.08	4.08	0.06	1.77073	2.77335	4.07136	10.000	1.1535	0.0428	0.055	0.3267	0.0297
28	5638	1.65	0.04	2.840	0.07	4.64	0.04	1.70255	2.98770	4.52232	19.953	0.0000	0.0428	0.011	0.3663	0.0000
29	5812	1.70	0.04	3.055	0.08	4.81	0.04	1.66446	3.15871	4.67995	19.953	0.0000	0.1528	0.022	0.3663	0.0000
30	5813	1.42	0.07	2.675	0.09	4.65	0.05	1.54169	2.92077	4.43947	19.953	0.0000	-0.0012	0.011	0.3564	0.0050
31	5831	2.00	0.05	3.045	0.06	4.38	0.03	1.97884	3.06244	4.38225	6.310	2.1885	0.3508	0.099	0.3663	0.0050
32	5846	1.45	0.07	2.860	0.08	4.93	0.04	1.48289	3.12627	4.62969	19.953	0.0000	0.1308	0.022	0.3564	0.0000
33	6127	1.50	0.05	2.845	0.11	4.96	0.06	1.48289	3.12627	4.62969	19.953	0.0000	0.1308	0.022	0.3564	0.0049
34	6702	2.46	0.06	2.995	0.08	3.80	0.04	2.43345	3.00445	3.80248	1.778	0.0965	0.5928	0.044	0.3267	0.0149
35	6703	1.88	0.06	2.925	0.07	4.30	0.04	1.89739	2.91066	4.29724	10.000	2.4550	0.1528	0.110	0.3663	0.0049
36	7052	1.48	0.07	2.835	0.11	5.02	0.06	1.47326	3.16048	4.66121	19.953	0.0000	0.1528	0.022	0.3564	0.0049
37	7454	2.15	0.06	2.475	0.08	3.27	0.05	2.15648	2.47821	3.27696	3.981	0.7320	-0.0232	0.044	0.1980	0.0346
38	7562	1.69	0.05	2.865	0.07	4.54	0.03	1.71883	2.91906	4.45813	19.953	0.0000	-0.0012	0.011	0.3663	0.0000
39	7619	1.36	0.04	3.055	0.08	5.06	0.03	1.43477	3.29732	4.78727	19.953	0.0000	0.2408	0.011	0.3564	0.0000
40	7626	1.46	0.05	2.825	0.07	5.05	0.03	1.47326	3.16048	4.66121	19.953	0.0000	0.1528	0.011	0.3564	0.0000
41	7785	1.63	0.06	2.915	0.08	4.60	0.04	1.70255	2.98770	4.52232	19.953	0.0000	0.0428	0.022	0.3663	0.0049

Table B.2. Solutions for the Trager "ID SP pristine" sample obtained using the Mean Recursive Minimum Distance Method.

Num.	Name	Age	[Z=H]	Age = Fe]	Num.	Name	Age	[Z=H]	Age = Fe]
1	A 569A	10.000	0.19313	0.21780	63	NGC 3923	17.783	0.53413	0.32340
2	IC 1696	10.000	0.34347	0.21120	64	NGC 4008	12.589	0.17113	0.19635
3	IC 2555	8.913	0.21513	0.18645	65	NGC 4033	6.310	0.10513	0.22110
4	NGC 194	8.913	0.22247	0.17490	66	NGC 4073	7.079	0.43147	0.29535
5	NGC 221	3.981	-0.05620	0.24420	67	NGC 4121	17.783	-0.24687	0.36630
6	NGC 227	8.913	0.46080	0.26400	68	NGC 4261	17.783	0.64413	0.23100
7	NGC 548	15.849	0.09780	0.35805	69	NGC 4283	8.913	0.19680	0.32835
8	NGC 584	11.220	0.19313	0.20790	70	NGC 4308	8.913	-0.14787	0.36465
9	NGC 596	10.000	0.11247	0.20955	71	NGC 4339	7.943	0.18947	0.22275
10	NGC 636	4.467	0.24080	0.19800	72	NGC 4342	10.000	0.37647	0.19800
11	NGC 687	12.589	0.46813	0.27225	73	NGC 4365	7.079	0.57080	0.27225
12	NGC 720	6.310	0.64413	0.32010	74	NGC 4387	14.125	0.03547	0.33990
13	NGC 741	8.913	0.31413	0.16830	75	NGC 4406	19.953	0.43513	0.37290
14	NGC 821	8.913	0.24813	0.20625	76	NGC 4434	7.079	0.17480	0.18150
15	NGC 1016	17.783	0.57813	0.28215	77	NGC 4458	8.913	-0.15153	0.33990
16	NGC 1199	8.913	0.34713	0.22275	78	NGC 4464	17.783	-0.17720	0.32835
17	NGC 1273	10.000	0.36913	0.15840	79	NGC 4467	19.953	0.01713	0.37125
18	NGC 1283	3.981	0.53047	0.27390	80	NGC 4472	14.125	0.63313	0.26730
19	NGC 1293	15.849	0.46080	0.23595	81	NGC 4473	19.953	0.51580	0.34155
20	NGC 1339	17.783	0.39480	0.39930	82	NGC 4478	7.943	0.08313	0.21615
21	NGC 1374	7.079	0.26647	0.29370	83	NGC 4486B	12.589	0.11247	0.28545
22	NGC 1395	11.220	0.46080	0.28050	84	NGC 4489	4.467	-0.04153	0.33000
23	NGC 1399	11.220	0.58180	0.19470	85	NGC 4551	11.220	0.13447	0.25080
24	NGC 1400	10.000	0.53780	0.32010	86	NGC 4552	19.953	0.64413	0.20295
25	NGC 1404	12.589	0.53413	0.33165	87	NGC 4564	5.012	0.70280	0.09900
26	NGC 1521	3.981	0.33980	0.27555	88	NGC 4648	3.548	0.57447	0.41415
27	NGC 1537	3.162	0.32880	0.19470	89	NGC 4649	8.913	0.67713	0.20955
28	NGC 1573	5.012	0.51947	0.31845	90	NGC 4660	19.953	0.36180	0.21120
29	NGC 1600	19.953	0.55980	0.37125	91	NGC 4697	19.953	0.46447	0.28380
30	NGC 1700	3.548	0.39113	0.20295	92	NGC 4742	1.585	-0.15887	0.22935
31	NGC 2300	7.943	0.55613	0.32670	93	NGC 4760	17.783	0.16747	0.19635
32	NGC 2563	17.783	0.65880	0.16170	94	NGC 4786	12.589	0.40580	0.28050
33	NGC 2634	17.783	0.18213	0.23595	95	NGC 4789	8.913	0.42047	0.33990
34	NGC 2636	7.943	-0.10020	0.26895	96	NGC 4839	17.783	0.31780	0.21945
35	NGC 2672	19.953	0.63313	0.37125	97	NGC 4841A	7.943	0.46813	0.30360
36	NGC 2673	7.079	0.29580	0.18150	98	NGC 4841B	3.981	0.40580	0.34485
37	NGC 2693	19.953	0.57447	0.26895	99	NGC 4860	19.953	0.50480	0.36630
38	NGC 2832	6.310	0.67713	0.09570	100	NGC 4874	19.953	0.30313	0.28710
39	NGC 2863	1.995	-0.11853	0.20625	101	NGC 4886	19.953	0.02080	0.22605
40	NGC 2888	2.818	-0.11487	0.19470	102	NGC 4889	15.849	0.63680	0.38610
41	NGC 2986	19.953	0.64780	0.37125	103	NGC 4915	10.000	0.43880	0.27060
42	NGC 3078	5.623	0.48647	0.28380	104	NGC 4926	3.162	0.42413	0.22935
43	NGC 3090	8.913	0.46813	0.25575	105	NGC 4957	11.220	0.36180	0.26400
44	NGC 3091	15.849	0.49747	0.38775	106	NGC 5017	17.783	0.02813	0.17655
45	NGC 3115	19.953	0.54513	0.28050	107	NGC 5018	3.162	0.00980	0.16995
46	NGC 3156	1.259	-0.34953	0.36300	108	NGC 5061	1.585	0.42413	0.28050
47	NGC 3309	12.589	0.60013	0.31680	109	NGC 5129	15.849	0.17847	0.20130
48	NGC 3348	19.953	0.23347	0.19470	110	NGC 5198	7.943	0.34347	0.23925
49	NGC 3377	7.943	0.17113	0.18810	111	NGC 5322	5.623	0.38013	0.20955
50	NGC 3379	19.953	0.39847	0.24585	112	NGC 5328	7.079	0.36180	0.26400
51	NGC 3585	8.913	0.49380	0.26400	113	NGC 5557	3.162	0.54513	0.26730
52	NGC 3605	6.310	0.00247	0.35640	114	NGC 5582	14.125	0.18580	0.22110
53	NGC 3608	19.953	0.39847	0.19800	115	NGC 5629	12.589	0.06847	0.12870
54	NGC 3610	5.012	0.19680	0.19635	116	NGC 5812	7.079	0.66980	0.09900
55	NGC 3613	8.913	0.22247	0.20295	117	NGC 5831	5.012	0.36913	0.30690
56	NGC 3640	5.012	0.27013	0.19305	118	NGC 5982	7.079	0.33980	0.19800
57	NGC 3818	8.913	0.37647	0.35475	119	NGC 6086	3.981	0.56713	0.28215
58	NGC 3837	19.953	0.37280	0.19305	120	NGC 6127/8	17.783	0.57080	0.28380
59	NGC 3841	17.783	0.29947	0.23265	121	NGC 6411	7.079	0.22980	0.19635
60	NGC 3872	17.783	0.62213	0.24420	122	NGC 7454	6.310	-0.20287	0.34650
61	NGC 3872	7.943	0.26117	0.28760	123	NGC 7562	10.000	0.00112	0.25610